

1 **Response to the comments of Reviewer 1**

2  
3 **This article provides what I consider an obvious first-order approach to modeling the effect of**  
4 **polarization of scattered sunlight over bare/desert regions. The advantages of the model are**  
5 **that it is simple and straightforward and physically intuitive. I consider this to be the first step**  
6 **in more complicated models. In addition, the model does not shy away from using advanced**  
7 **techniques. For instance, the authors select the agglomerated debris particles to represent**  
8 **their atmospheric aerosols. These particles have been demonstrated to be the most accurate at**  
9 **modeling the light-scattering properties of dust particles. In fact, they are the ONLY model**  
10 **particles that can accurately reproduce the light-scattering properties at multiple wavelengths**  
11 **(Zubko, 2013). As an introductory paper to this complicated topic, the paper leaves open**  
12 **several lines for future research and discussion. Not only does it provide the foundation for**  
13 **future, more advanced modeling approaches, but leaves some research questions unanswered:**

14  
15 **Answer: The authors of this manuscript greatly thank this reviewer for the helpful and insightful**  
16 **comments.**

17  
18 **1. When more complicated surface models are incorporated, how will this effect the**  
19 **results?**

20  
21 **Answer: In the Conclusion, we add "When more complicated surface models such as that**  
22 **considering desert as semi-infinite particle layers are considered, it may improve the total**  
23 **reflectance modeling, but will have little effect on polarization degree and angle of**  
24 **polarization calculation, since polarization is mostly determined by single scattering at**  
25 **the top layer of the sand particles."**  
26

27 **2. As with any model that is composed of several distinct physical parts, what are the**  
28 **predominate sources of error and what observations are necessary to test these parts**  
29 **independently, so that we know where it is best to focus our efforts to make**  
30 **improvements?**

31  
32 **Answer: For a model composed of several distinct physical parts, the predominate**  
33 **sources of error is from each part. We must test each part and do sensitivity studies on the**  
34 **error effect of each part to determine the final error of the model. When we use**  
35 **observation data to check the error of each part, we must consider the sensitivity study of**  
36 **other parts, and use the representative parameters for other parts to model the final**  
37 **results, which are compared with the observational data.**  
38

39 **3. Most significant in my mind are the surface parameters  $f$  and  $\sigma$  and their lack of**  
40 **dependence. What happens, for instance, when we consider extreme incident angles?**

1  
2 Answer: the surface parameters  $f$  and  $\sigma$  are determined by the desert physical fact,  
3 which are fitted out by satellite data. They may have dependence on each other. But when  
4 they work together as a pair, they can produce results close to the satellite data. They are  
5 paired quantities and must be used as a pair. They should not be significantly affected by  
6 incident angles, but since they are derived from satellite data with limited incident angles,  
7 they may have small dependence on the incident angle due to sampling issue.  
8

9 ***My only significant criticism is that I would prefer to see the figures discussed in more depth.***  
10 ***The authors present several of these and make broad statements. In the text, they really should***  
11 ***state what each figure shows and why it is being presented.***

12 Answer: There are many figures with similar natures in the manuscript to better show the results  
13 for different wavelengths/viewing or incident geometries. Since we already have detailed  
14 description of each figure in the captions, we prefer to explain them in a summarized way in the  
15 text, to avoid redundant statements which make the paper lengthy. We tried our best to make the  
16 text concise under the condition that the meaning of each figure can be understood. Thanks for  
17 the reviewer's recommendation, but we think we want to keep the summarized way to make the  
18 article concise.  
19

20 ***There are some minor typographical considerations that I have transmitted to the authors.***

21 Answer: Great thanks to the reviewer for the very detailed corrections of our errors in the text. A  
22 lot of careful corrections were made. The authors really appreciate the great help from this  
23 reviewer.  
24

## 25 **Response to the comments of Reviewer 2**

26

27 ***This paper develops an algorithm for obtaining the spectral polarization state of solar light***  
28 ***from desert with the PARASOL data. Through numerical experiments, concise but***  
29 ***meaningful results are summarized. The reviewer recommends the publication to ACP, but the***  
30 ***minor points below should be addressed before the publication.***  
31

32 Answer: The authors of this manuscript thank this reviewer for the helpful comments.

33 The manuscript has been revised rigorously following these comments.  
34

1 *1) In Introduction, the importance of polarization correction should be emphasized*  
2 *quantitatively to let readers know the importance of this subject. How about adding some*  
3 *sentences around L15-17 in P8527.*

4  
5 Answer: This is done. We add "For example, the PARASOL data show that the degree of  
6 polarization (DOP) of reflected light from clear-sky desert can be ~30%. The broad-leaf trees  
7 also can reflect solar light with a DOP of ~70%. For a sensor with a sensitivity-to-polarization  
8 factor of only ~1%, its measurement for light with a DOP of ~30% and ~70% will have relative  
9 errors of ~0.3% and ~0.7%, respectively, solely due to the polarization (Sun and Lukashin,  
10 2013)." in this section.

11  
12 *2) In Method of L17 in P8530, how is the sensitivity of the assumption for 0.02 of the*  
13 *refractive index?*

14  
15 Answer: We add "This assumption of sand's imaginary refractive index could have a small effect  
16 on the modeled total reflectance from the desert, but has little effect on the DOP and AOLP  
17 calculations." in the text.

18  
19 *3) For typographical point, L11 in P8535, 'Figures 20 to 15', 15 should be 25.*

20  
21 Answer: This is corrected.

1 **Deriving Polarization Properties of Desert-Reflected Solar Spectra**  
2 **with PARASOL Data**

3  
4 Wenbo Sun<sup>1\*</sup>, Rosemary R. Baize<sup>2</sup>, Constantine Lukashin<sup>2</sup>, and Yongxiang Hu<sup>2</sup>

5  
6 <sup>1</sup>Science Systems and Applications Inc., Hampton, VA, 23666, USA

7 <sup>2</sup>NASA Langley Research Center, Hampton, VA, 23681, USA

8 \*Mail Stop 420, NASA Langley Research Center, Hampton, VA, 23681

9 [wenbo.sun-1@nasa.gov](mailto:wenbo.sun-1@nasa.gov)

10  
11  
12  
13 ~~Revised Submitted for~~ Atmospheric Chemistry and Physics

14  
15 ~~June~~ **February 18<sup>0</sup>, 2015**

16  
17  
18  
19 

---

Corresponding author address: Wenbo Sun, Mail Stop 420, NASA Langley Research Center, 21  
20 Langley Boulevard, Hampton, VA, 23681-2199. E-mail: [wenbo.sun-1@nasa.gov](mailto:wenbo.sun-1@nasa.gov)

1 **Highlights**

- 2       **1.** Spectral polarization state of reflected solar radiation is needed in correcting satellite  
3           data.
- 4       **2.** An algorithm for deriving spectral polarization state of solar light from desert is reported.
- 5       **3.** PARASOL data at 3 polarized channels are used in deriving polarization of whole solar  
6           spectra.
- 7       **4.** Desert-reflected solar light's polarization state at any wavelength can be obtained.

8

9

10

11

12

13

14

15

16

17

18

19

20

21

1 **Abstract.** One of the major objectives of the Climate Absolute Radiance and Refractivity  
2 Observatory (CLARREO) is to conduct highly accurate spectral observations to provide an on-  
3 orbit inter-calibration standard for relevant Earth-observing sensors with various channels. To  
4 calibrate an Earth-observing sensor's measurements with the highly accurate data from the  
5 CLARREO, errors in the measurements caused by the sensor's sensitivity to the polarization  
6 state of light must be corrected. For correction of the measurement errors due to the light's  
7 polarization, both the instrument's dependence ~~to~~ on the incident ~~tee's~~ polarization states ~~us~~ and the  
8 on-orbit knowledge of the polarization state of light as a function of observed scene type,  
9 viewing geometry, and solar wavelength, are required. In this study, an algorithm for deriving  
10 the spectral polarization state of solar light from desert is reported. The desert/bare land surface  
11 is assumed to be composed of two types of areas: Fine sand grains with diffuse reflection  
12 (Lambertian non-polarizer) and quartz-rich sand particles with facets of various orientations  
13 (specular-reflection polarizer). The adding-doubling radiative transfer model (ADRTM) is  
14 applied to integrate the atmospheric absorption and scattering in the system. Empirical models  
15 are adopted in obtaining the diffuse spectral reflectance of sands and the optical depth of the dust  
16 aerosols over the desert. The ratio of non-polarizer area to polarizer area and the angular  
17 distribution of the facet orientations are determined by fitting the modeled polarization states of  
18 light to the measurements at 3 polarized channels (490, 670, and 865 nm) by the Polarization and  
19 Anisotropy of Reflectances for Atmospheric Science instrument coupled with Observations from  
20 a Lidar (PARASOL). Based on this physical model of the surface, the desert-reflected solar  
21 light's polarization state at any wavelength in the whole solar spectra can be calculated with the  
22 ADRTM.

1 **Key words:** Desert, radiation polarization, solar spectra, inter-calibration, CLARREO,  
2 PARASOL.

3

#### 4 **1 Introduction**

5 One of the major objectives of the Climate Absolute Radiance and Refractivity Observatory  
6 (CLARREO) (Wielicki *et al.*, 2013) is to conduct highly accurate spectral observations to  
7 provide an on-orbit inter-calibration standard for relevant Earth-observing sensors with various  
8 channels. To calibrate an Earth-observing sensor's measurements with the highly accurate data  
9 from the CLARREO, errors in the measurements caused by the sensor's sensitivity to the  
10 polarization state of light must be corrected (Lukashin *et al.*, 2013; Sun and Lukashin, 2013; Sun  
11 *et al.*, 2015). For correction of the measurement errors due to light's polarization, both the  
12 instrument's dependence on the incident light's polarization state and the on-orbit knowledge of  
13 the polarization state of light as a function of observed scene type, viewing geometry, and solar  
14 wavelength, are required. Empirical polarization distribution models (PDMs) (Nadal and Breon,  
15 1999; Maignan *et al.*, 2009) based on data from the Polarization and Anisotropy of Reflectances  
16 for Atmospheric Science instrument coupled with Observations from a Lidar (PARASOL)  
17 (Deschamps *et al.*, 1994) may be used to correct radiometric bias (Lukashin *et al.*, 2013). But  
18 these can only be done at ~~3~~ 4 solar wavelengths (i.e. 490, 670, and 865 nm) at which the  
19 PARASOL has reliable polarization measurements. Since the CLARREO is designed to measure  
20 solar spectra from 320 to 2300 nm with a spectral sampling of 4 nm (Wielicki *et al.*, 2013),  
21 which has potential to inter-calibrate space-borne sensors at nearly all of the solar wavelengths  
22 (Sun and Lukashin, 2013), the PDMs for the inter-calibration applications should be made as  
23 functions of every sampling wavelength of the CLARREO. Due to strong dependence of solar

1 light's polarization on wavelength (Sun and Lukashin, 2013), the applicability of empirical  
2 PDMs based on only 3 ~~or 4~~ channels of PARASOL polarization measurements will be very  
3 limited. In our previous studies (Sun and Lukashin, 2013; Sun *et al.*, 2015), polarized solar  
4 radiation from the ocean-atmosphere system is accurately modeled. Because the refractive index  
5 of water at solar spectra is well known (Thormählen et al., 1985), *Sun and Lukashin* (2013)  
6 actually can produce the PDMs for ocean-atmosphere system at any solar wavelength. However,  
7 it is still a difficult problem to obtain spectral PDMs for other scene types. For scene types other  
8 than water bodies, although many studies have been conducted (Coulson et al., 1964; Egan,  
9 1968; Egan 1969; Wolff, 1975; Egan, 1970; Vanderbilt and Grant, 1985; Tamalge and Curran,  
10 1986; Grant, 1987), no reliable surface reflection matrix such as that based on the Cox and Munk  
11 (1954; 1956) wave slope distribution models for oceans is available. For scene types dominated  
12 by diffuse reflection, like fresh snow, grass lands or needle-leaf trees/bushes, this may not be a  
13 serious problem. But for scene types like desert, snow crust/ice surfaces, or even broad-leaf trees,  
14 specular reflection is still significant (like what happens at the ocean surface), polarization of the  
15 reflected light can be very strong, thus needs to be accurately accounted for. For example, the  
16 PARASOL data show that the degree of polarization (DOP) of reflected light from clear-sky  
17 desert can be ~30%. The broad-leaf trees also can reflect solar light with a DOP of ~70%. For a  
18 sensor with a sensitivity-to-polarization factor of only ~1%, its measurement for light with a  
19 DOP of ~30% and ~70% will have relative errors of ~0.3% and ~0.7%, respectively, solely due  
20 to the polarization (Sun and Lukashin, 2013).

21 For bare soils and vegetation, Breon et al. (1995) developed some simple methods to calculate  
22 the polarized reflectance from the surface. But these methods can only model the polarized  
23 reflectance, which are not suitable for deriving the full elements of the surface reflection matrix

1 for coupling with the radiative transfer model to simulate all Stokes parameters of the reflected  
 2 light at the top of the atmosphere (TOA). Our objective for this study is to model the PDMs,  
 3 which are [the](#) degree of polarization (DOP) and angle of linear polarization (AOLP) (Sun and  
 4 Lukashin, 2013) of the reflected light at any solar wavelength. Polarized reflectance solely is  
 5 insufficient for deriving the DOP and not usable for deriving the AOLP.

6 In this study, an algorithm for obtaining the spectral polarization state of solar light from desert  
 7 with the PARASOL data is developed. The method of deriving the polarization state of solar  
 8 light from desert-atmosphere system at any wavelength with the PARASOL-measured polarized  
 9 radiances at 490, 670, and 865 nm is reported in Section 2. Numerical results and discussions are  
 10 presented in Section 3. Summary and conclusions are given in Section 4.

## 11 **2 Method**

12 The polarization of reflected light is related to the surface roughness (Wolff, 1975) and to the  
 13 size of reflecting elements (Egan, 1970). In this study, the desert/bare land surface is assumed to  
 14 be composed of two types of areas: Fine sand grains with diffuse reflection (Lambertian non-  
 15 polarizer) and quartz-rich sand particles with facets of various orientations (specular-reflection  
 16 polarizers). The desert surface light reflection matrix is obtained based on mixed effects of the  
 17 two types of areas. Similar to the treatment for rough-ocean surfaces (e.g. Sun and Lukashin,  
 18 2013), the desert surface reflection matrix with 4x4 elements is calculated as

$$19 \quad \mathbf{R}_0(\theta_s, \theta_v, \varphi) = f\mathbf{R}_L + (1 - f) \frac{\pi \mathbf{M}(\theta_s, \theta_v, \varphi)}{4 \cos^4 \beta \cos \theta_s \cos \theta_v} P(Z_x, Z_y), \quad (1)$$

20 where  $\theta_s$ ,  $\theta_v$ , and  $\varphi$  denote solar zenith angle, viewing zenith angle, and relative azimuth angle  
 21 of the reflected light, respectively. The fraction of Lambertian area is denoted as  $f$ .  $\mathbf{R}_L$  is the  
 22 reflection matrix of Lambertian reflector, with the reflectance as the only nonzero element. The

1 4x4 elements of  $\mathbf{M}(\theta_s, \theta_v, \varphi)$  for each quartz-rich sand particle facet orientation are calculated in  
2 the same way as in Mishchenko and Travis (1997) based on the Fresnel Laws.  $P(Z_x, Z_y)$  is the  
3 quartz-rich sand facet orientation probability distribution as a function of the surface roughness.  
4 Assuming desert is a stationary sand “ocean” with quartz-rich sand particle facets as specular-  
5 reflection “waves” and Lambertian reflection sand grains as “foams”, we can adopt the formula  
6 given in Cox and Munk (1956) for  $P(Z_x, Z_y)$  as

$$7 \quad P(Z_x, Z_y) = \frac{1}{\pi\sigma^2} \exp\left(-\frac{Z_x^2 + Z_y^2}{\sigma^2}\right), \quad (2)$$

8 where  $\sigma$  denotes the roughness parameter of the desert surface, and

$$9 \quad Z_x = \frac{\partial Z}{\partial x} = \frac{\sin \theta_v \cos \varphi - \sin \theta_s}{\cos \theta_v + \cos \theta_s}, \quad (3)$$

$$10 \quad Z_y = \frac{\partial Z}{\partial y} = \frac{\sin \theta_v \sin \varphi}{\cos \theta_v + \cos \theta_s}. \quad (4)$$

11 In Eqs. (2) to (4),  $Z$  denotes the height of the surface. In Eq. (1),  $\beta$  is the tilting angle of a sand  
12 facet, and  $\tan \beta = \sqrt{Z_x^2 + Z_y^2}$ .

13 The polarization of reflected solar radiation from the Earth-atmosphere system is the result of  
14 both the surface reflection and the scattering by molecules and particles in the atmosphere. In  
15 this study, the adding-doubling radiative-transfer model (ADRTM) (Sun and Lukashin, 2013) is  
16 applied to integrate the atmospheric absorption and scattering with the desert surface reflection.

17 To get the reflection matrix elements of desert with Eq. (1), we must obtain 4 unknown quantities  
18 in advance:  $f$ ,  $\sigma$ ,  $\mathbf{R}_L$ , and the refractive index of quartz-rich sand. In this study, the refractive  
19 index of quartz-rich sand is assumed to be that of fused silica as a function of solar wavelength  
20 (Malitson, 1965):

$$n^2 - 1 = \frac{0.6961663\lambda^2}{\lambda^2 - (0.0684043)^2} + \frac{0.4079426\lambda^2}{\lambda^2 - (0.1162414)^2} + \frac{0.8974794\lambda^2}{\lambda^2 - (9.896161)^2}, \quad (5)$$

where  $n$  is the real refractive index of the silica and  $\lambda$  denotes the solar wavelength in  $\mu\text{m}$ . In this study, to account for the impurity absorption in the quartz-rich sands, we assume the imaginary part of the sand refractive index to be 0.02. This assumption of sand's imaginary refractive index could have a small effect on the modeled total reflectance from the desert, but has little effect on the DOP and AOLP calculations.

However,  $f$ ,  $\sigma$ , and  $\mathbf{R}_L$  must be obtained from observations for desert. In this study, the spectral structure of the Lambertian reflectance of desert  $R_L^0(\lambda)$  for wavelength longer than 800 nm is based on the analysis of data in *Aoki et al. (2002)* and *Sadiq and Howari (2009)* for desert reflectance in Taklimakan Desert and the southeast of Qatar, respectively. For wavelengths shorter than 800 nm, the spectral structure of  $R_L^0(\lambda)$  is determined by an analysis of data in *Aoki et al. (2002)*, *Sadiq and Howari (2009)*, *Bowker et al. (1985)*, and *Koelemeijer et al. (2003)*. This spectral reflectance structure multiplied with a scale factor  $\alpha$  is then entered in the ADRTM, and on the condition of  $f = 1.0$  and at a solar zenith angle of  $28.77^\circ$  the solar reflectances at the wavelength of 490, 670, and 865 nm from the ADRTM and those from the 24-day mean of the PARASOL measurements are compared. ByWith varying the scale factor  $\alpha$ , we can make the reflectances at the wavelengths of 490, 670, and 865 nm from the ADRTM close to those from the PARASOL data. The resultant  $\alpha R_L^0(\lambda)$  is the reflectance of the Lambertian desert area, which as the first element of the  $\mathbf{R}_L$ , is linearly extrapolated to the CLARREO solar wavelength limit of 320 nm. The empirical spectral reflectance of desert from this process is displayed in Fig. 1.

Since desert reflectance varies significantly with desert types (*Otterman, 1981; Bowker et al., 1985; Dobber et al., 1998; Aoki et al., 2002; Koelemeijer et al., 2003*), our empirical desert  $\mathbf{R}_L$

1 model may ~~not~~ be ~~not~~ very representative. However, with the other two free parameters  $f$  and  $\sigma$  in  
2 the model, we may still approach ~~the~~ accurate PDMs (i.e. DOP and AOLP) even when  $\mathbf{R}_L$  has  
3 some difference from true values in practice.

4 In this study, the ~~adding-doubling radiative transfer model~~ (ADRTM) (Sun and Lukashin, 2013)  
5 is applied for calculation of the Stokes parameters of the reflected light from the desert-  
6 atmosphere system. The U. S. Standard Atmosphere (1976) is applied in the calculations. Gas  
7 absorption coefficients from the  $k$ -distribution treatment (Kato *et al.*, 1999) of the spectral data  
8 from the line-by-line radiative transfer model (LBLRTM) (Clough *et al.*, 1992; 1995) using the  
9 MODTRAN 3 dataset (Kneizys *et al.*, 1988) is used. Ozone absorption coefficients are taken  
10 from the ozone cross-section table provided by the World Meteorological Organization (1985)  
11 for wavelengths smaller than 700 nm. Molecular scattering optical thickness is from *Hansen and*  
12 *Travis* (1974). The scattering phase-matrix elements of molecular atmosphere are based on ~~the~~  
13 Rayleigh scattering solution with a depolarization factor of 0.03 (Hansen and Travis, 1974).  
14 Single-scattering properties of sand-dust aerosols are ~~calculated using agglomerated debris~~  
15 ~~particles with~~ ~~from~~ the discrete-dipole approximation (DDA) light scattering model (Zubko *et*  
16 *al.*, 2006; 2009; 2013). Two-mode lognormal size distributions (Davies, 1974; Whitby, 1978;  
17 Reist, 1984; Ott, 1990; Porter and Clarke, 1997) are applied in calculation of the single-  
18 scattering properties of aerosols. A dust aerosol refractive index of  $1.5 + 0.0i$  is assumed in the  
19 modeling. An average aerosol optical depth (AOD) of the dust over the Morocco desert  
20 (Toledano *et al.*, 2008) is adopted in this study:

$$21 \quad AOD = 0.2374\lambda^{-0.2291}, \quad (6)$$

22 where  $\lambda$  is the solar wavelength in  $\mu\text{m}$ . Dust AOD decreases with the increase of wavelength.

23 In this study, the ratio of ~~the~~ non-polarizer area to polarizer area of the desert and the angular

1 distribution of the quartz-rich sand—particle facet orientations are determined by fitting the  
2 modeled polarization states of reflected light to the measurements at 3 polarized channels (490,  
3 670, and 865 nm) by the PARASOL. By varying the two free parameters  $f$  and  $\sigma$  in the model,  
4 we calculated a lookup table of spectral DOP and AOLP as functions of  $f$  and  $\sigma$  for desert. We  
5 then compared the modeled DOP and AOLP with those from the PARASOL data. The pair of  $f$   
6 and  $\sigma$  that simultaneously produce similar DOP and AOLP to the PARASOL data at a solar  
7 zenith angle of  $28.77^\circ$  and 3 polarized channels (490, 670, and 865 nm) of the PARASOL are the  
8 retrieved values for the physical model of desert surface. In this retrieval, the PARASOL data are  
9 from the mean of 24-day measurements for global desert. The 24 days of PARASOL data are  
10 taken from the first two days of each month across 2006. The retrieved  $f$  and  $\sigma$  values are then  
11 used to calculate the DOP and AOLP at any solar wavelengths and any solar zenith angles. This  
12 can produce the PDMs for clear-sky desert. For desert with clouds, it is straightforward to do the  
13 calculation [bywith](#) simply adding cloud layers in the ADRTM.

14

### 15 **3 Results**

16 In this study, the retrieved values of  $f$  and  $\sigma$  for desert are 0.95 and 0.164, respectively. These  
17 values are applied to the ADRTM to calculate the polarization properties of reflected solar  
18 spectra from desert. Figures 2 to 4 show the modeled reflectance, DOP, and AOLP of reflected  
19 solar light from desert at a wavelength of 490 nm and a solar zenith angle (SZA) of  $28.77^\circ$  with  
20 those from the PARASOL data at a SZA bin of  $27\text{-}30^\circ$ . We can see that the model results are  
21 very close to the PARASOL data at nearly all viewing directions. The modeled DOP agrees very  
22 well with that from the PARASOL data, with differences [s](#) smaller than 5%. The AOLPs from the  
23 ADRTM and the PARASOL are also very similar, with only minor differences at viewing angles

1 close to the backscattering direction. The reflectance from the ADRTM with  $f = 0.95$  and  $\sigma =$   
2 0.164 is also very close to that from the PARASOL, which is nearly Lambertian but a little larger  
3 at backward-reflecting directions. At a larger SZA of  $56.94^\circ$ , Figures 5 to 7 show that the  
4 modeled reflectance, DOP, and AOLP are also very close to those from the PARASOL data,  
5 demonstrating that the retrieved desert physical property  $f = 0.95$  and  $\sigma = 0.164$  work well for  
6 solar angles other than the SZA of  $28.77^\circ$ , at which they are derived from the PARASOL  
7 measurements. From Figs. 2-7, we also can see that at the wavelength of 490 nm desert has [a](#)  
8 strong polarization effect in the forward-reflecting direction. At a viewing zenith angle (VZA) of  
9  $60^\circ$ , the DOP of desert at 490 nm can reach  $\sim 30\%$ , which means that for a satellite sensor with  
10 only  $\sim 1\%$  polarization dependence, the desert polarization to sunlight can cause  $\sim 0.3\%$  error in  
11 spectral radiance measurement (Sun and Lukashin, 2013).

12 For a longer wavelength of 670 nm, Figures 8 to 13 show that the modeled DOP is [very](#)  
13 [similarwell-close](#) to the PARASOL data for different solar and viewing angles. The AOLP from  
14 the ADRTM shows some difference from that of the PARASOL at backward-reflecting  
15 directions. Particularly, Figure 10 shows that the AOLP from the ADRTM has a pattern in the  
16 neighborhood of backward-reflecting angle that is very similar to those for clouds reported in  
17 *Sun and Lukashin (2013)*, *Sun et al. (2014)*, and *Sun et al. (2015)*. This [likely isis](#) because ~~that~~  
18 the refractive index for dust aerosols in our modeling is assumed to be 1.5 and the imaginary part  
19 is zero. Under this condition, the dust particles are nonabsorbing crystals which have similar  
20 scattering properties to water droplets or ice crystals in clouds at the wavelength of 670 nm.  
21 However, it [is's](#) worth noting here that the errors in the AOLP from the ADRTM due to our  
22 assumptions for dust refractive index will only have [a](#) minor effect on the polarization correction  
23 accuracy. This is due to the fact that the DOPs at these observation angles are very small, and

1 also that the AOLP errors in these observation angles actually will not result in any significant  
2 difference in polarization correction, i.e. AOLP =  $\sim 0^\circ$  and AOLP =  $\sim 180^\circ$  means the same to the  
3 satellite sensor. However, at 670 nm, the PARASOL data for desert show stronger reflectance in  
4 the backward-reflecting directions than in the forward-reflecting directions. This is significantly  
5 different from the ocean cases. Desert's reflection ~~of the~~ solar radiation is a complicated  
6 ~~phenomenon~~ ~~issue that which~~ is neither Lambertian nor specular-reflection. Thus, our simple  
7 approach here shows some difference in reflectance from ~~the~~ data. However, our objective for  
8 this study is to ~~accurately~~ model the desert DOP accurately, and to ~~accurately~~ model the desert  
9 AOLP accurately when the DOP is not trivial. Such modeling errors in the total reflectance are to  
10 be expected and not the concern of this study. ~~Errors in modeling the reflectance is ignorable for~~  
11 ~~this purpose.~~

12 For an even longer wavelength of 865 nm, Figures 14 to 19 show that, similar to the cases for the  
13 wavelength of 670 nm, the modeled DOP and AOLP are very ~~similar~~ ~~close~~ to the PARASOL  
14 data. The PARASOL reflectance at 865 nm also shows significantly stronger reflectance in the  
15 backward-reflecting directions than in the forward-reflecting directions. Without knowing the  
16 proper reason for the desert reflectance angular feature, our modeling cannot capture this angular  
17 distribution of reflected light well. This is a topic deserving further study, probably by  
18 researchers concerned with ~~This is worthy of being studied by people working for the~~ radiation  
19 energy budget studies.

20 Note here that it is not a surprise that we can get accurate modeling ~~for of~~ the DOP and AOLP of  
21 reflected solar spectra from desert as shown in Figs. 2-4, 8-10, and 14-16, for a solar zenith angle  
22 of  $28.77^\circ$ , since the parameters  $f = 0.95$  and  $\sigma = 0.164$  used in the modeling are retrieved from the  
23 PARASOL data at this solar zenith angle. To examine whether or not the desert surface physical

1 parameters ( $f$  and  $\sigma$ ) from a specific solar zenith angle can be accurately applied to any other  
2 solar zenith angles, we modeled the polarized radiation from the desert-atmosphere system at a  
3 solar zenith angle of  $56.94^\circ$  with the  $f$  and  $\sigma$  obtained at a solar zenith angle of  $28.77^\circ$ . These  
4 modeling results are compared with the PARASOL data in Figs. 5-7, 11-13, and 17-19. It is  
5 demonstrated that at all the 3 wavelengths of 490, 670, and 865 nm, the DOP and AOLP from  
6 the ADRTM agree well with the PARASOL data in every case. These results show that the  
7 method can be applied to any other solar zenith angles once the desert surface physical  
8 parameters ( $f$  and  $\sigma$ ) are obtained at a specific solar zenith angle.

9 As mentioned previously, the CLARREO is designed to measure solar spectra from 320 to 2300  
10 nm with a spectral sampling of 4 nm. To calibrate space-borne sensors with the CLARREO  
11 measurements in the solar spectra, the PDMs to correct polarization-induced errors in  
12 radiation measurement for the inter-calibration applications should be made as a function of  
13 every sampling wavelength of the CLARREO. Therefore, the modeling of the reflected solar  
14 radiation's polarization must be done over the range of solar wavelengths. Figures 20 to  
15 25 show exemplary results for the modeling method to be applied to the wavelength limits  
16 (320 nm and 2300 nm) of the CLARREO solar measurements at different solar zenith angles. It  
17 is shown that at short wavelengths, the region's polarization from desert regions to solar  
18 radiation is can be very strong, can be ~50%. However, But at long wavelengths region, desert's  
19 the polarization degree is only ~10%. However But even a ~10% degree of polarization degree  
20 could cause significant errors in radiance if the sensor's dependence on polarization is  
21 significant.

22

## 23 4 Conclusions

1 In this study, an algorithm for deriving [the](#) spectral polarization state of solar light [reflected](#) from  
2 desert is reported. The desert/bare land surface is assumed to be composed of two types of areas:  
3 Fine sand grains with diffuse reflection (Lambertian non-polarizer) and quartz-rich sand particles  
4 with facets of various orientations (specular-reflection polarizer). The ~~adding doubling radiative~~  
5 ~~transfer model~~ (ADRTM) is applied to integrate the atmospheric absorption and scattering in the  
6 system. Empirical models are adopted in obtaining the diffuse spectral reflectance of sands and  
7 the optical depth of the dust aerosols over the desert. The ratio of non-polarizer area to polarizer  
8 area and the angular distribution of the facet orientations are determined by fitting the modeled  
9 polarization states of light to the measurements at 3 polarized channels (490, 670, and 865 nm)  
10 by the ~~Polarization and Anisotropy of Reflectances for Atmospheric Science instrument coupled~~  
11 ~~with Observations from a Lidar~~ (PARASOL). Based on this [simple](#) physical model of [the](#)  
12 surface, [the polarization state of the](#) desert-reflected solar ~~light's polarization state~~ radiation at  
13 any wavelength in the whole solar spectra can be calculated with the ADRTM. When more  
14 complicated surface models such as that considering desert as semi-infinite particle layers are  
15 considered, it may improve the total reflectance modeling, but will have little effect on  
16 polarization degree and angle of polarization calculation, since polarization is mostly determined  
17 by single scattering at the top layer of the sand particles.

18

19

20

21 **Acknowledgment**

1 This work is supported by NASA's CLARREO mission. The authors thank Bruce A. Wielicki  
2 for this support and helpful discussions.

3

#### 4 **References**

- 5 1. Aoki, T., Mikami, M., and Liu, W.: Spectral albedos of desert surfaces and size  
6 distributions of soil particles measured around Qira and Aksu in the Taklimakan Desert,  
7 *J. Arid Land Studies*, 11, 259–266, 2002.
- 8 2. Bowker, D., Davis, R., Myrick, D., Stacy, K., and Jones, W.: Spectral reflectances of  
9 natural targets for use in remote sensing studies, NASA RP-1139, NASA Langley  
10 Research Center, Hampton, Virginia, USA, 1985.
- 11 3. Bréon, F.-M., Tanré, D., Lecomte, P., and Herman, M.: Polarized reflectance of bare soils  
12 and vegetation: measurements and models, *IEEE Trans. Geosci. Remote Sens.*, 33, 487-  
13 499, 1995.
- 14 4. Clough, S. A., Iacono, M. J., and Moncet, J.-L.: Line-by-line calculation of atmospheric  
15 fluxes and cooling rates: Application to water vapor, *J. Geophys. Res.*, 97, 15761-15785,  
16 1992.
- 17 5. Clough, S. A., and Iacono, M. J.: Line-by-line calculations of atmospheric fluxes and  
18 cooling rates II: Application to carbon dioxide, ozone, methane, nitrous oxide, and the  
19 halocarbons, *J. Geophys. Res.*, 100, 16,519-16,535, 1995.
- 20 6. Coulson, K. L., Gray E. L., and Bouricius, G. M.: A study of the reflection and  
21 polarization characteristics of selected natural and artificial surfaces, *Tech. Informat.*  
22 *Series*, Rep. R64SD74, General Electric Co., Space Sciences Laboratory, Philadelphia,  
23 Pennsylvania, USA, 1964.

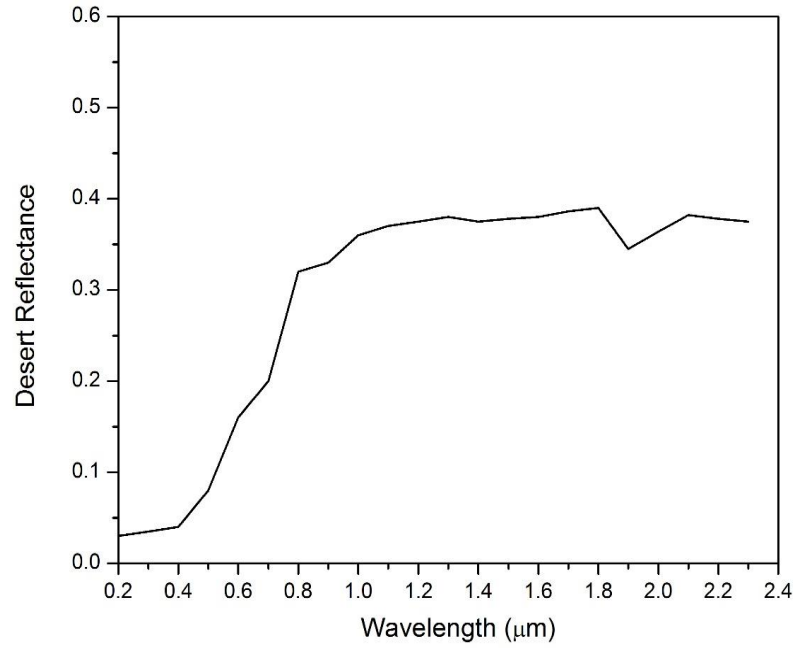
- 1 7. Cox, C., and Munk, W.: Measurement of the roughness of the sea surface from  
2 photographs of the sun's glitter, *J. Opt. Soc. Amer.*, 44, 838-850, 1954.
- 3 8. Cox. C., and Munk, W.: Slopes of the sea surface deduced from photographs of sun  
4 glitter, *Bull. Scripps Inst. Oceanogr.*, 6, 401-488, 1956.
- 5 9. Davies, C.: Size distribution of atmospheric particles, *Aerosol Science*, 5, 293–300, 1974.
- 6 10. Deschamps, P. Y., Bréon, F. M., Leroy, M., Podaire, A., Bricaud, A., Buriez, J. C., and  
7 Sèze, G.: The POLDER mission: Instrument characteristics and scientific objectives,  
8 *IEEE Trans. Geosci. Remote Sens.*, 32, 598–615, 1994.
- 9 11. Dobber, M., Goede, A., and Burrows, J.: Observations of the moon by the global ozone  
10 monitoring spectrometer experiment: radiometric calibration and lunar albedo, *Appl.*  
11 *Opt.*, 37, 7832–7841, 1998.
- 12 12. Egan, W. G.: Aircraft polarimetric and photometric observations, *Proc. 5th Int. Symp.*  
13 *Remote Sensing Env.*, 169-189, Environmental Research Institute of Michigan, Ann  
14 Arbor, Michigan, USA, April 16-18, 1968
- 15 13. Egan, W. G.: Polarimetric and photometric simulation of the Martian surface, *Icarus*, 10,  
16 223-227, 1969.
- 17 14. Egan, W. G.: Optical stokes parameters for farm crops identification, *Remote Sens.*  
18 *Env.*, 1, 165 -180, 1970.
- 19 15. Hansen, J. E., and Travis, L. D.: Light scattering in planetary atmospheres, *Space Sci.*  
20 *Rev.*, 16, 527-610, doi:10.1007/BF00168069, 1974.
- 21 16. Kato, S., Ackerman, T. P., Mather, J. H., and Clothiaux, E. E.: The k-distribution method  
22 and correlated-k approximation for a shortwave radiative transfer model, *J. Quant.*  
23 *Spectrosc. Radiat. Trans.*, 62, 109-121, doi: 10.1016/S0022-4073(98)00075-2, 1999.

- 1 17. Kneizys, F. X., Shettle, E. P., Abreu, L. W., Chetwynd, J. H., Anderson, G. P., Gallery,  
2 W. O., Selby, J. E. A., and Clough, S. A.: *Users guide to LOWTRAN 7*, AFGL-TR-88-  
3 0177, Optical/Infrared Technology Division, Airforce Geophysics Division,  
4 Massachusetts, USA, 1988.
- 5 18. Koelemeijer, R., de Haan, J., and Stammes, P.: A database of spectral surface reflectivity  
6 in the range 335-772 nm derived from 5.5 years of GOME observations, *J. Geophys.*  
7 *Res.*, 108, No. D2, 4070, doi: 10.1029/2002JD002429, 2003.
- 8 19. Lukashin, C., Wielicki, B.A., Young, D.F., Thome, K., Jin, Z., and Sun, W.: Uncertainty  
9 estimates for imager reference inter-calibration with CLARREO reflected solar  
10 spectrometer, *IEEE Trans. Geosci. Rem. Sens. special issue on intercalibration of*  
11 *satellite instruments*, 51, 1425-36, 2013.
- 12 20. Maignan, F., Breon, F.-M., Fedele, E., and Bouvier, M.: Polarized reflectances of natural  
13 surfaces: Spaceborne measurements and analytical modeling, *Remote Sens. Environ.*,  
14 113, 2642–2650, 2009.
- 15 21. Mishchenko, M. I., and Travis, L. D.: Satellite retrieval of aerosol properties over the  
16 ocean using polarization as well as intensity of reflected sunlight, *J. Geophys. Res.*, 102,  
17 16989-17013, doi: 10.1029/96JD02425, 1997.
- 18 22. Nadal, F., and Breon, F.-M.: Parameterization of surface polarized reflectance derived  
19 from POLDER spaceborne measurements, *IEEE Transac. Geosci. Remote Sens.*, 37,  
20 1709–1718, 1999.
- 21 23. National Oceanic and Atmospheric Administration, National Aeronautics and Space  
22 Administration, and United States Air Force: *U.S. Standard Atmosphere*, NOAA-S/T 76-  
23 1562, U.S. Government Printing Office, Washington, D.C., 1976.

- 1 24. Ott, W.: A physical explanation of the lognormality of pollutant concentrations, *J. Air*  
2 *Waste Manage. Assoc.*, 40, 1378–1383, 1990.
- 3 25. Otterman, J.: Satellite and field studies of man’s impact on the surface in arid regions,  
4 *Tellus*, 33, 68-77, 1981.
- 5 26. Porter, J. N., and Clarke, A. D.: Aerosol size distribution models based on in situ  
6 measurements, *J. Geophys. Res.*, 102, 6035-6045, 1997.
- 7 27. Reist, P. C.: *Introduction to Aerosol Science*, McMillan, New York, 1984.
- 8 28. Sadiq, A., and Howari, F.: Remote sensing and spectral characteristics of desert sand  
9 from Qatar Peninsula, Arabian/Persian Gulf, *Remote Sens.*, 1, 915-933, doi:  
10 10.3390/rs1040915, 2009.
- 11 29. Sun, W., and Lukashin, C.: Modeling polarized solar radiation from ocean-atmosphere  
12 system for CLARREO inter-calibration applications, *Atmos. Chem. Phys.*, 13, 10303-  
13 10324, doi: 10.5194/acp-13-10303-2103, 2013.
- 14 30. Sun, W., Videen, G., and Mishchenko, M. I.: Detecting super-thin clouds with polarized  
15 sunlight, *Geophys. Res. Lett.*, 41, 688-693, doi: 10.1002/2013GL058840, 2014.
- 16 31. Sun, W., Lukashin, C., Baize, R.R., and Goldin, D.: Modeling polarized solar radiation  
17 for CLARREO inter-calibration applications: Validation with PARASOL data, *J. Quant.*  
18 *Spectrosc. Radiat. Transfer*, 150, 121-133, 2015.
- 19 32. Toledano, C., Wiegner, M., Garhammer, M., Seefeldner, M., Gasteiger, J., Muller, D.,  
20 and Koepke, P.: Spectral aerosol optical depth characterization of desert dust during  
21 SAMUM 2006, *Tellus B*, 61, 216-228, 2008.
- 22 33. Tamalge, D. A., and Curran, P. J.: Remote sensing using partially polarized light, *Int. J.*  
23 *Remote Sens.*, 7, 47 -64, 1986.

- 1 34. Thormählen, I., Straub, J., Grigull, U.: Refractive index of water and its dependence on  
2 wavelength, temperature, and density, *J. Phys. Chem. Ref. Data*, 14, 933-945, 1985.
- 3 35. Vanderbilt, V. C., and Grant, L.: Plant canopy specular reflectance model, *IEEE Trans.*  
4 *Geosc. Remote Sens.*, 23, 722 -730, 1985.
- 5 36. Whitby, K.: The physical characteristics of sulfur aerosols, *Atmos. Environ.*, 12, 135–  
6 159, 1978.
- 7 37. Wielicki, B. A., Young, D. F., Mlynczak, M. G., Thome, K. J., Leroy, S., Corliss, J.,  
8 Anderson, J. G., Ao, C. O., Bantges, R., Best, F., Bowman, K., Brindley, H., Butler, J. J.,  
9 Collins, W., Doelling, D. R., Dykema, J. A., Feldman, D. R., Fox, N., Holz, R. E.,  
10 Huang, X., Huang, Y., Jennings, D. E., Jin, Z., Johnson, D. G., Jucks, K., Kato, S., Kirk-  
11 Davidoff, D. B., Knuteson, R., Kopp, G., Kratz, D. P., Liu, X., Lukashin, C., Mannucci,  
12 A. J., Phojanamongkolkij, N., Pilewskie, P., Ramaswamy, V., Revercomb, H., Rice, J.,  
13 Roberts, Y., Roithmayr, C. M., Rose, F., Sandford, S., Shirley, E. L., Smith, Sr., W. L.,  
14 Soden, B., Speth, P. W., Sun, W., Taylor, P. C., Tobin, D., and Xiong, X.: Climate  
15 absolute radiance and refractivity observatory (CLARREO): Achieving climate change  
16 absolute accuracy in orbit, *Bull. Amer. Meteor. Soc.*, 94, 1519-1539, doi: 10.1175/BAMS  
17 -D-12-00149.1, 2013.
- 18 38. Wolff, M.: Polarization of light reflected from rough planetary surface, *Appl.*  
19 *Opt.*, 14, 1395 -1405, 1975.
- 20 39. World Meteorological Organization: *Atmospheric ozone 1985*, Global ozone research and  
21 monitoring project, World Meteorological Organization (WMO) Report No. 16, Geneva,  
22 1985.

- 1 40. Zubko, E., Shkuratov, Y., Kiselev, N. N., and Videen, G.: DDA simulations of light  
2 scattering by small irregular particles with various structure, *J. Quant. Spectrosc. Radiat.*  
3 *Trans.*, 101, 416–434, 2006.
- 4 41. Zubko, E., Kimura, H., Shkuratov, Y., Muinonen, K., Yamamoto, T., Okamoto, H., and  
5 Videen, G.: Effect of absorption on light scattering by agglomerated debris particles, *J.*  
6 *Quant. Spectrosc. Radiat. Trans.*, 110, 1741–1749, 2009.
- 7 42. Zubko, E., Muinonen, K., Munoz, O., Nousiainen, T., Shkuratov, Y., Sun, W., Videen,  
8 G.: Light scattering by feldspar particles: Comparison of model agglomerate debris  
9 particles with laboratory samples, *J. Quant. Spectrosc. Radiat. Trans.*, 131, 175-187,  
10 2013.
- 11  
12  
13  
14  
15  
16  
17  
18



1

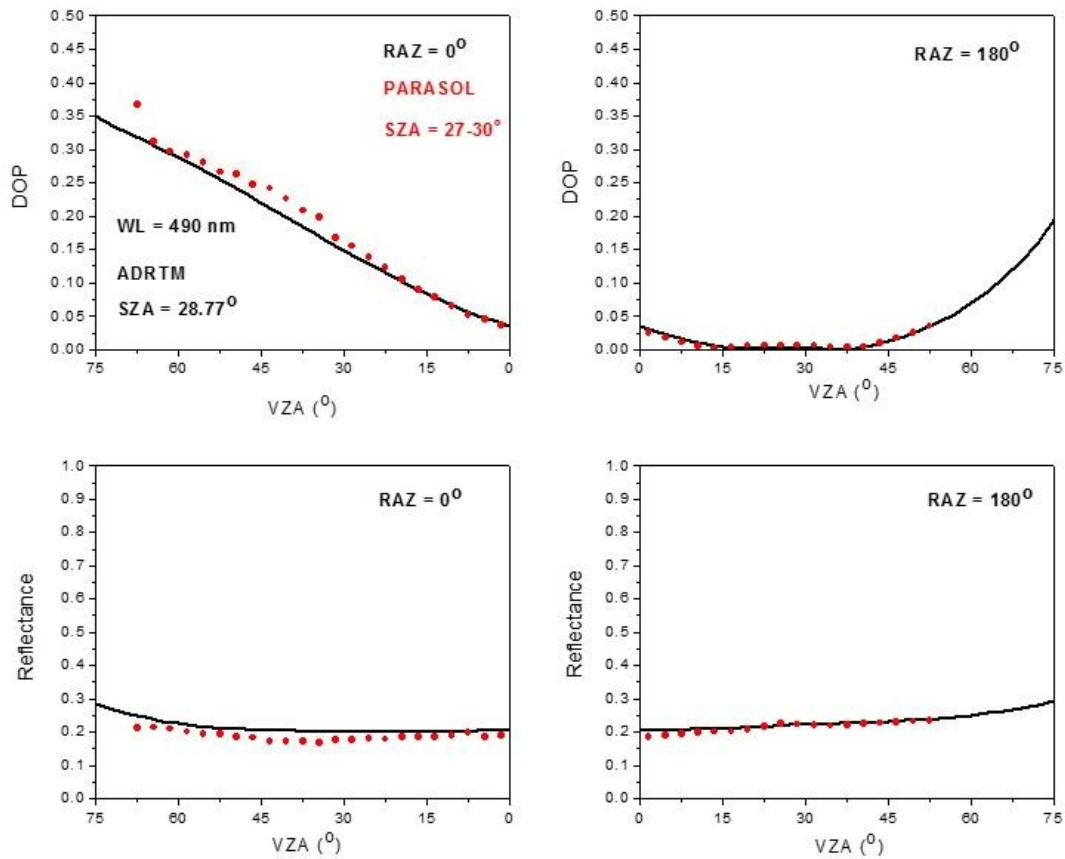
2 **Figure 1. Empirical spectral reflectance of desert from analysis of data in Aoki et al. (2002),**  
3 **Sadiq and Howari (2009), Bowker et al. (1985), and Koelemeijer et al. (2003), and is scaled**  
4 **by the PARASOL measurements.**

5

6

7

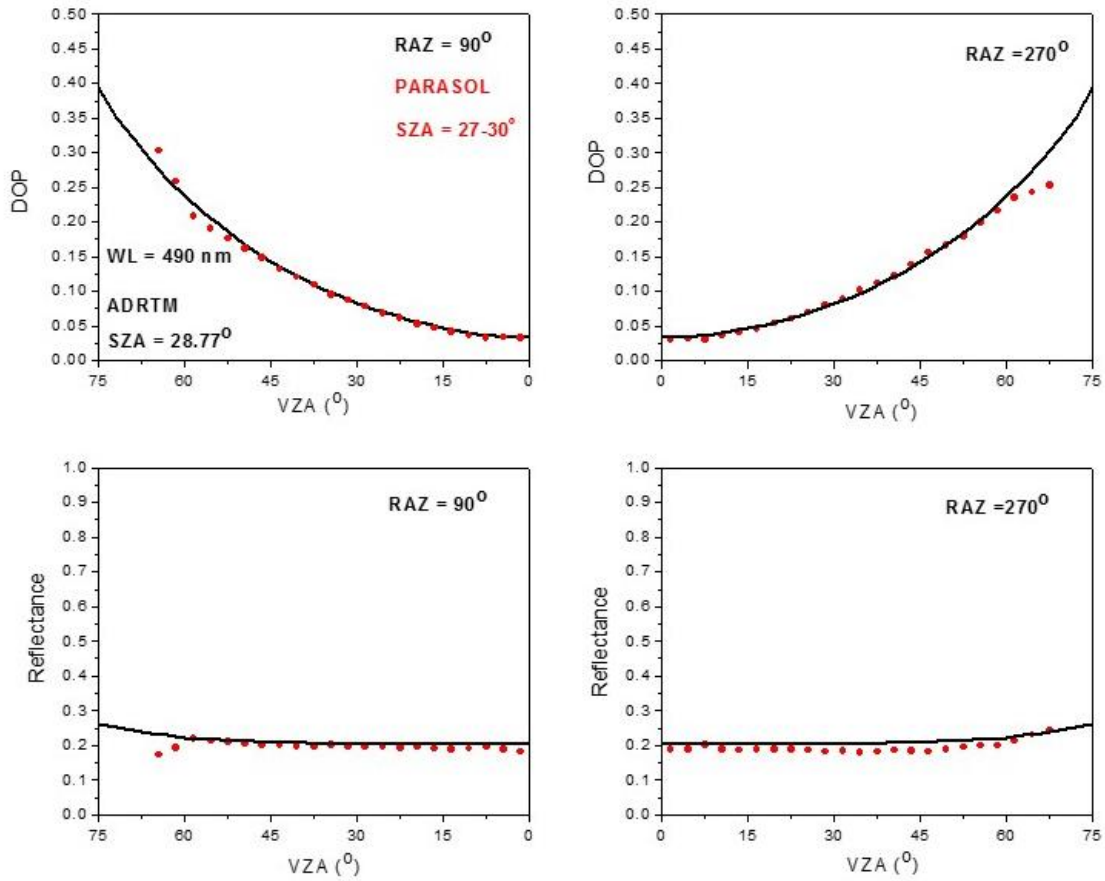
8



1  
2  
3  
4  
5  
6  
7  
8  
9

**Figure 2. Comparison of the modeled DOP and reflectance of desert-reflected solar light at relative azimuth angles (RAZ) of 0° and 180° with those from the PARASOL data at the wavelength of 490 nm. The solar zenith angle (SZA) is 28.77° in the modeling. The SZA is in the bin of 27-30° for the PARASOL data.**

1



2

3

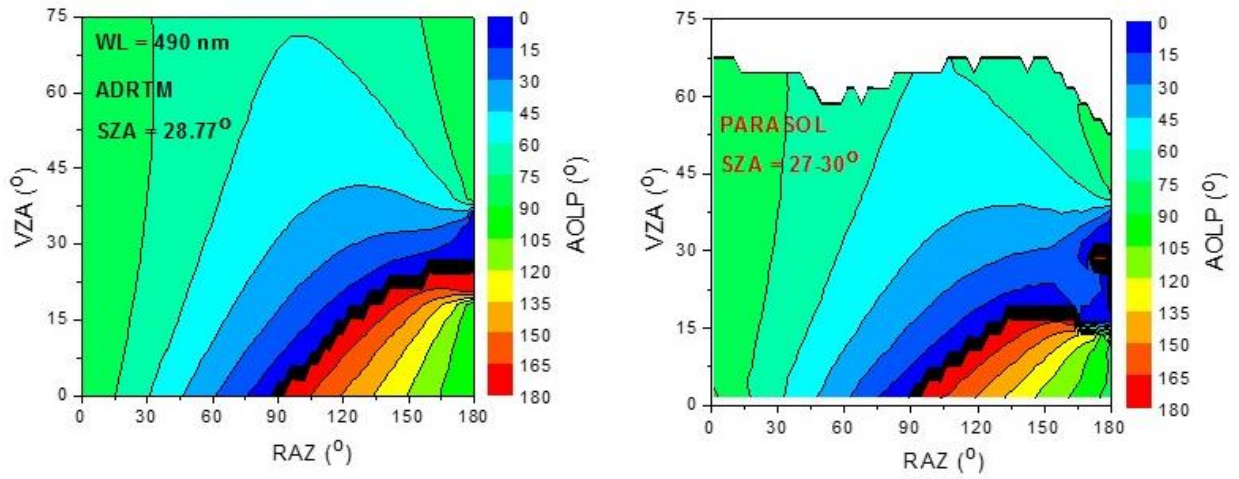
4

5 **Figure 3. Same as in Fig. 2, but at relative azimuth angles (RAZ) of 90° and 270°.**

6

7

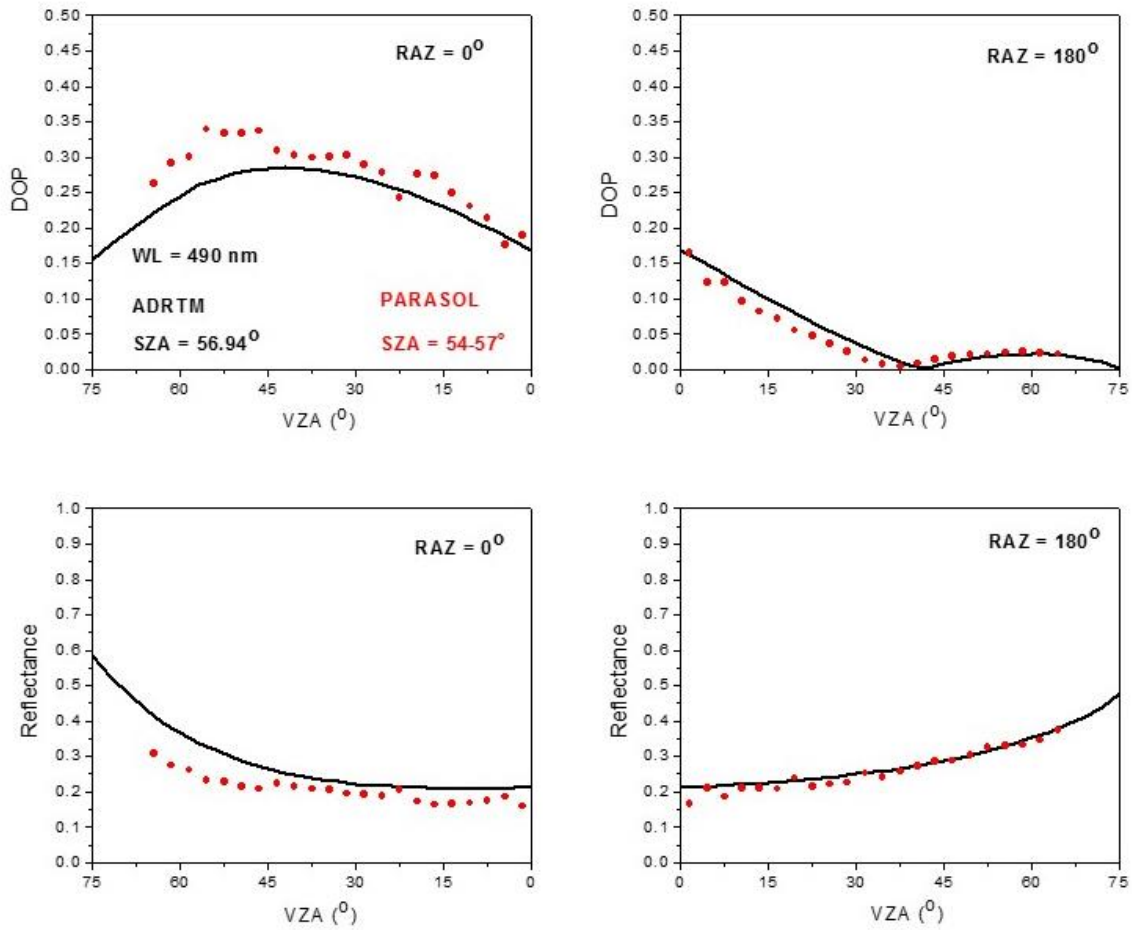
1  
2  
3  
4



5  
6

7 **Figure 4. Comparison of the modeled AOLP of desert-reflected solar light with those from**  
8 **the PARASOL data at the wavelength of 490 nm. The solar zenith angle (SZA) is 28.77° in**  
9 **the modeling. The SZA is in the bin of 27-30° for the PARASOL data.**

10  
11  
12  
13  
14



1

2 **Figure 5. Comparison of the modeled DOP and reflectance of desert-reflected solar light at**  
 3 **relative azimuth angles (RAZ) of 0° and 180° with those from the PARASOL data at the**  
 4 **wavelength of 490 nm. The solar zenith angle (SZA) is 56.94° in the modeling. The SZA is**  
 5 **in the bin of 54-57° for the PARASOL data.**

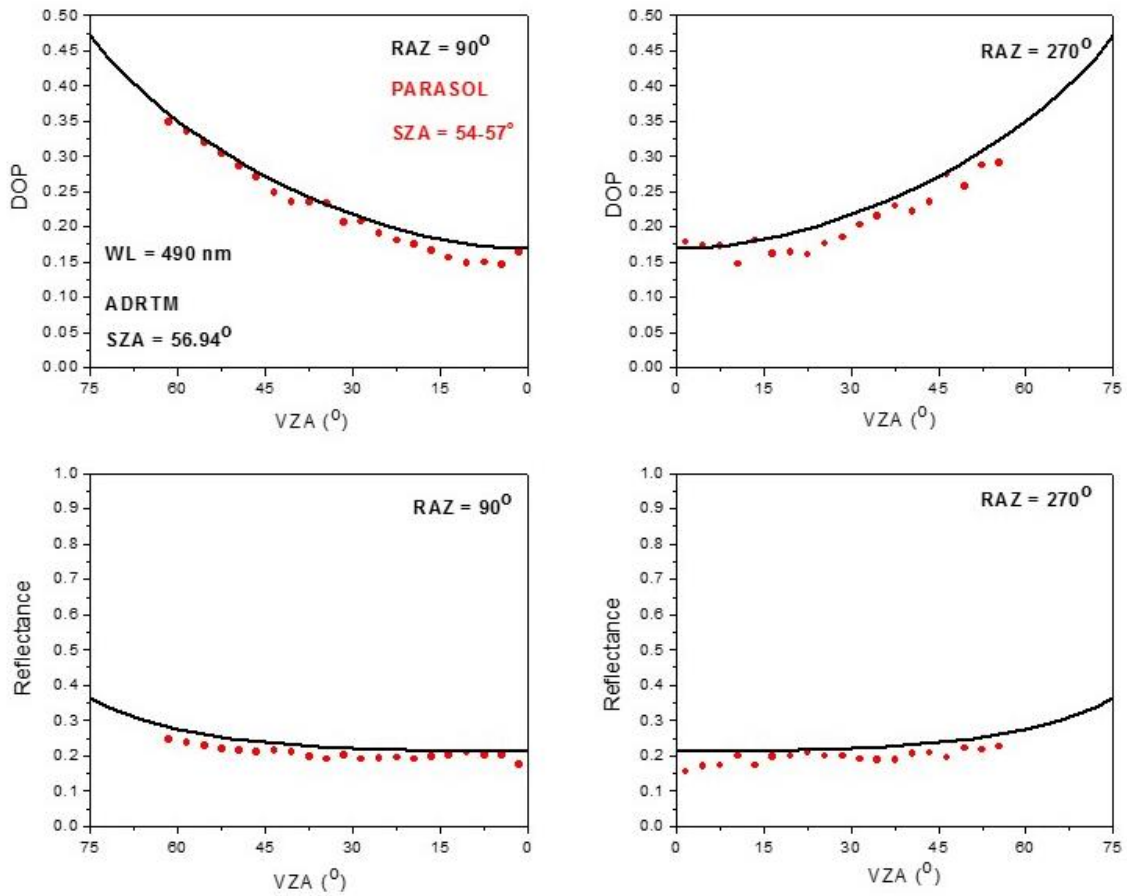
6

7

8

1

2



3

4 **Figure 6. Same as in Fig. 5, but at relative azimuth angles (RAZ) of 90° and 270°.**

5

6

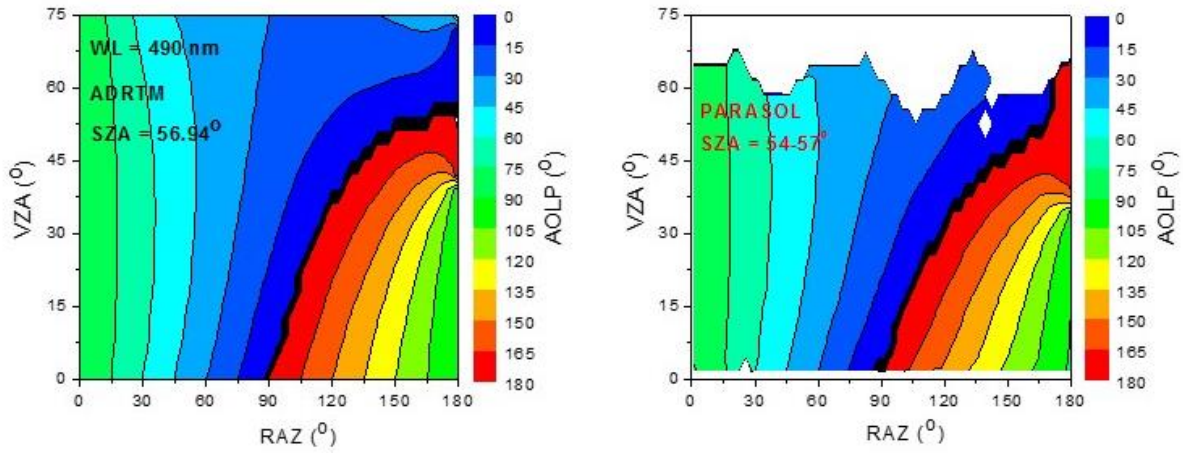
7

8

1

2

3



4

5

6

7 **Figure 7. Comparison of the modeled AOLP of desert-reflected solar light with those from**  
8 **the PARASOL data at the wavelength of 490 nm. The solar zenith angle (SZA) is 56.94° in**  
9 **the modeling. The SZA is in the bin of 54-57° for the PARASOL data.**

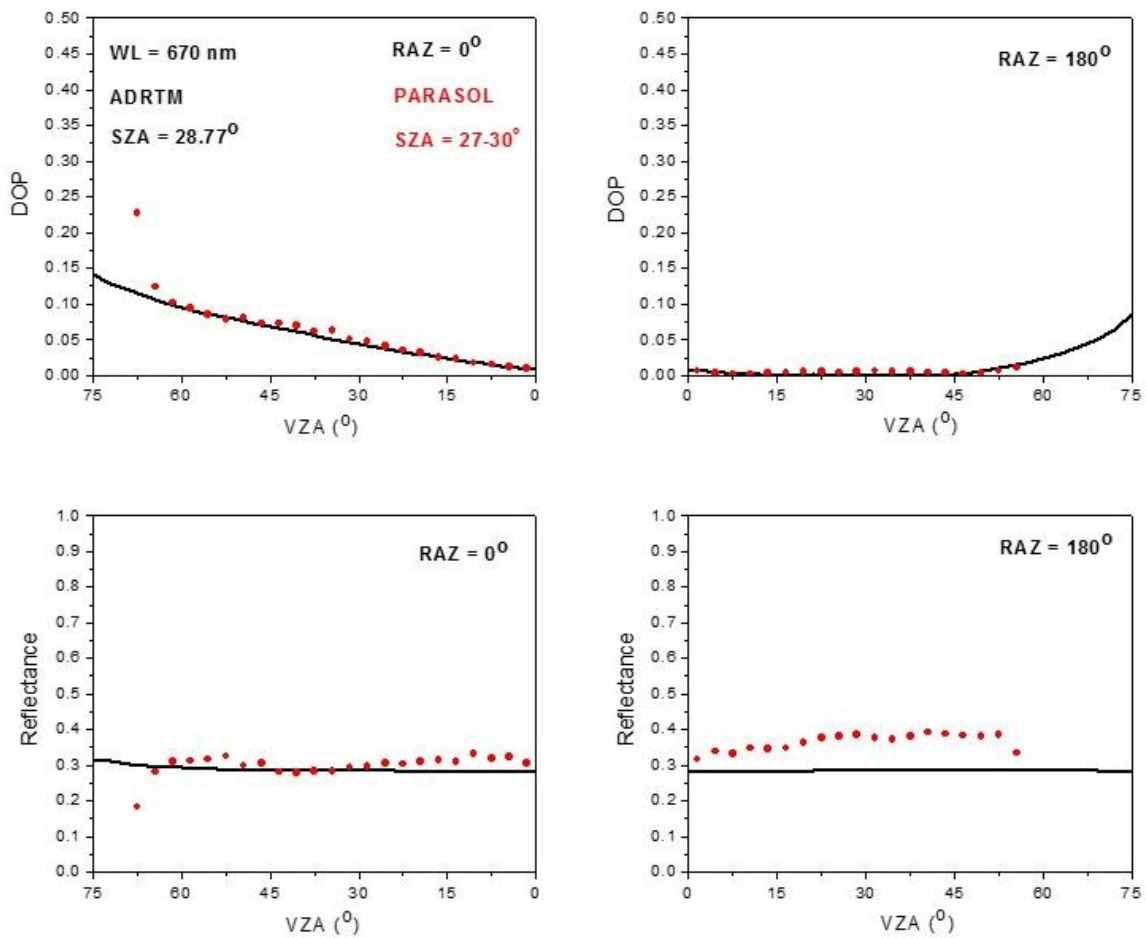
10

11

12

13

1



2

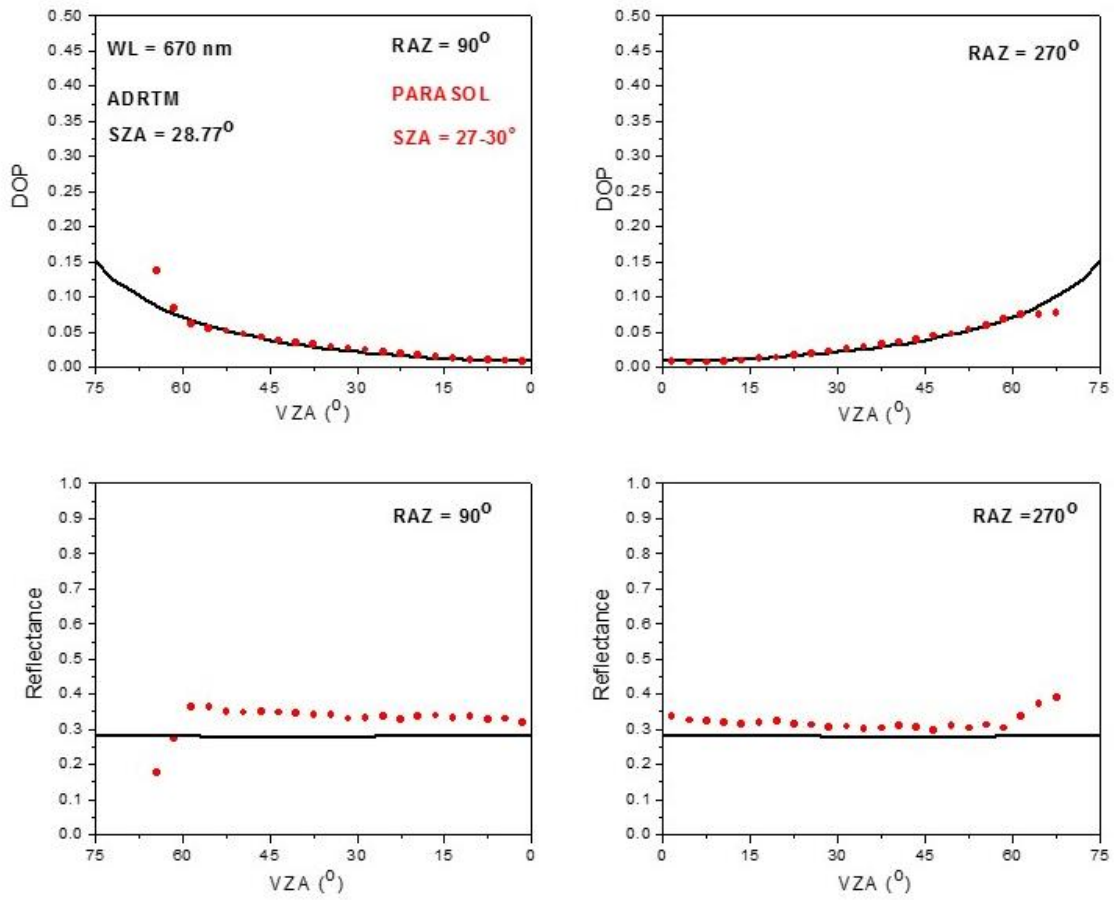
3

4 **Figure 8. Comparison of the modeled DOP and reflectance of desert-reflected solar light at**  
5 **relative azimuth angles (RAZ) of 0° and 180° with those from the PARASOL data at the**  
6 **wavelength of 670 nm. The solar zenith angle (SZA) is 28.77° in the modeling. The SZA is**  
7 **in the bin of 27-30° for the PARASOL data.**

8

9

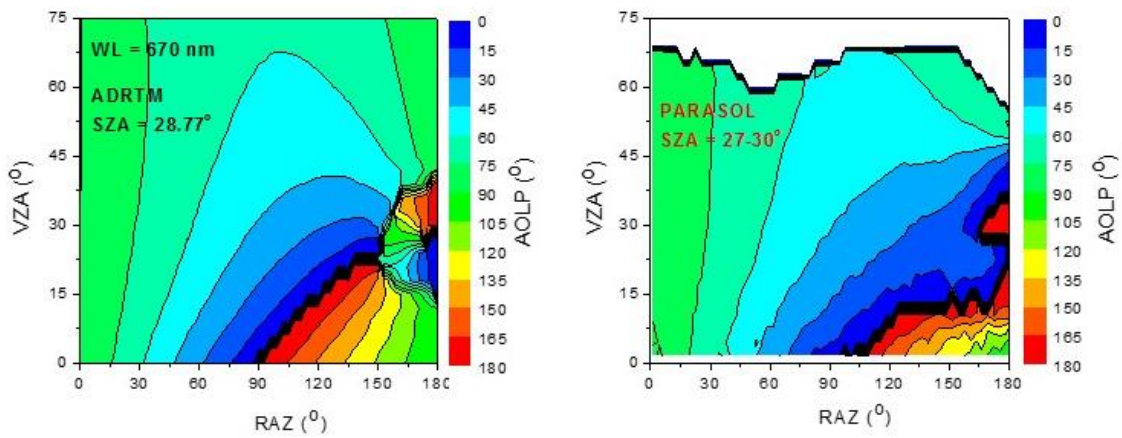
1  
2  
3  
4



5  
6  
7  
8

Figure 9. Same as in Fig. 8, but at relative azimuth angles (RAZ) of 90° and 270°.

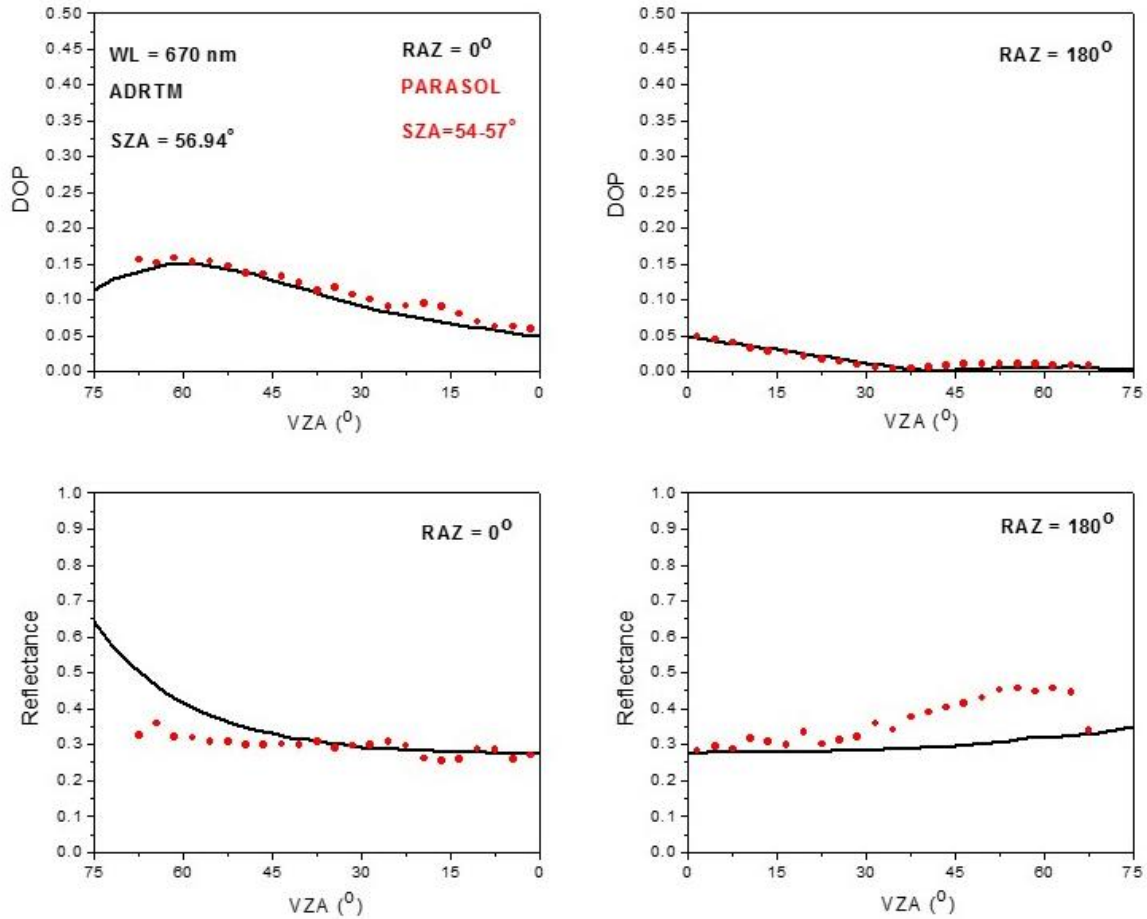
1  
2  
3  
4  
5  
6



7  
8  
9  
10  
11  
12  
13  
14  
15  
16

**Figure 10. Comparison of the modeled AOLP of desert-reflected solar light with those from the PARASOL data at the wavelength of 670 nm. The solar zenith angle (SZA) is 28.77° in the modeling. The SZA is in the bin of 27-30° for the PARASOL data.**

1



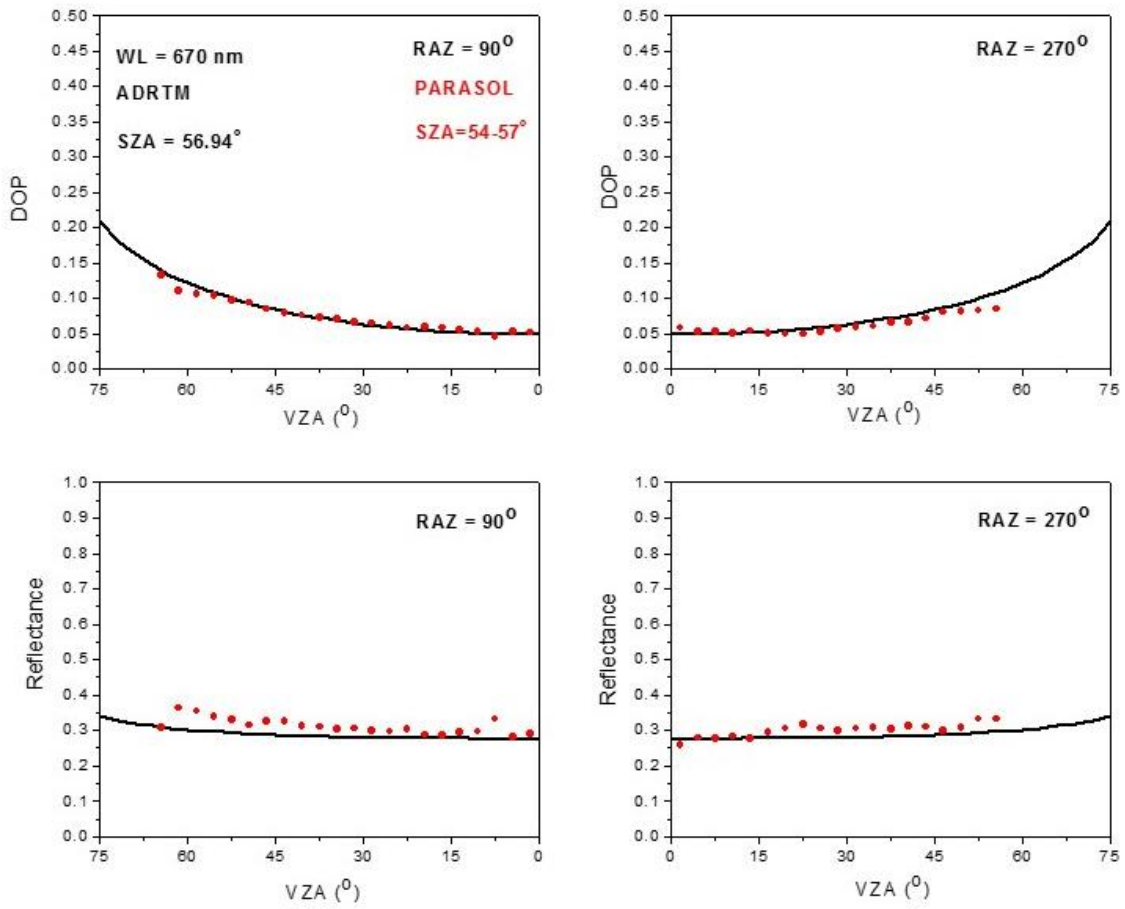
2

3

4

5 **Figure 11. Comparison of the modeled DOP and reflectance of desert-reflected solar light**  
6 **at relative azimuth angles (RAZ) of 0° and 180° with those from the PARASOL data at the**  
7 **wavelength of 670 nm. The solar zenith angle (SZA) is 56.94° in the modeling. The SZA is**  
8 **in the bin of 54-57° for the PARASOL data.**

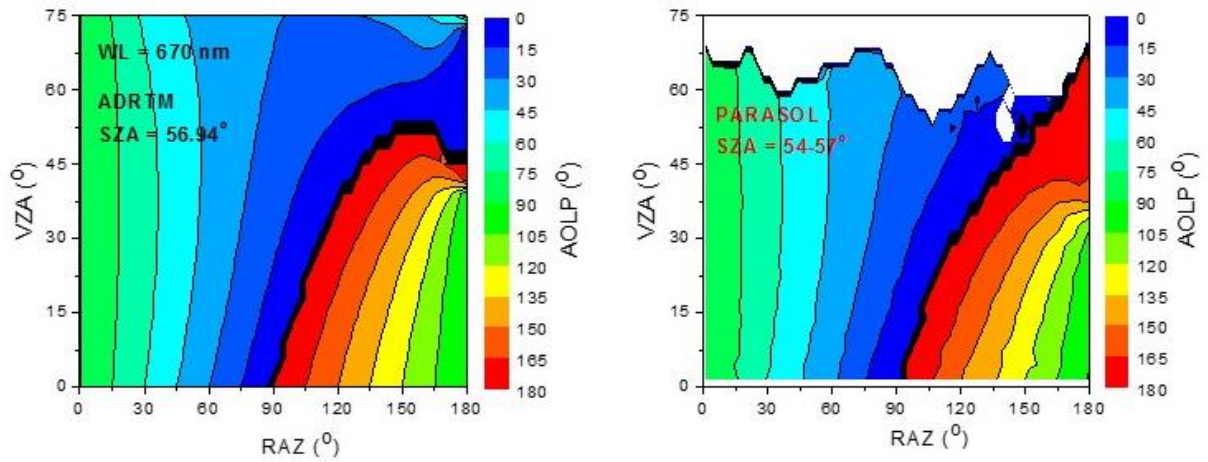
9



- 1
- 2
- 3
- 4
- 5
- 6
- 7
- 8
- 9

Figure 12. Same as in Fig. 11, but at relative azimuth angles (RAZ) of 90° and 270°.

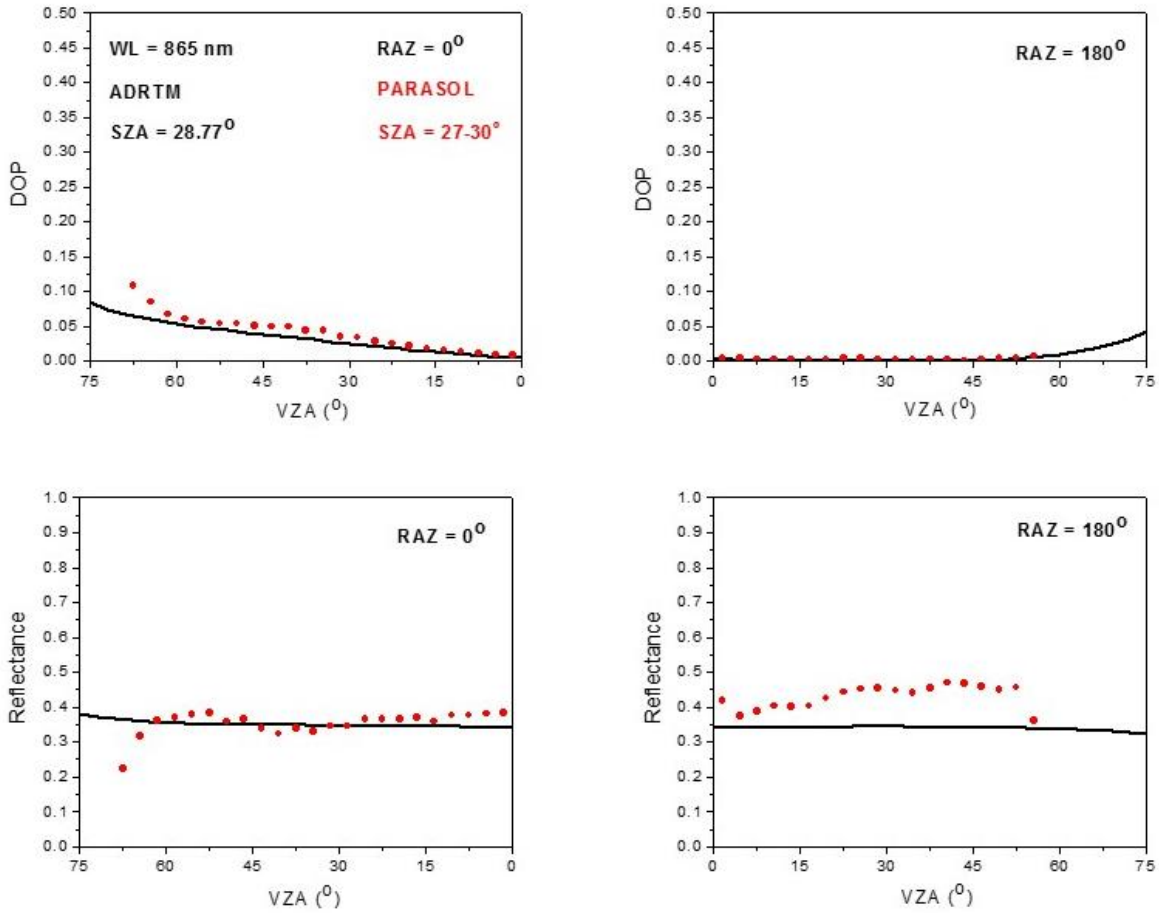
1  
2  
3  
4



5  
6  
7  
8  
9

**Figure 13. Comparison of the modeled AOLP of desert-reflected solar light with those from the PARASOL data at the wavelength of 670 nm. The solar zenith angle (SZA) is 56.94° in the modeling. The SZA is in the bin of 54-57° for the PARASOL data.**

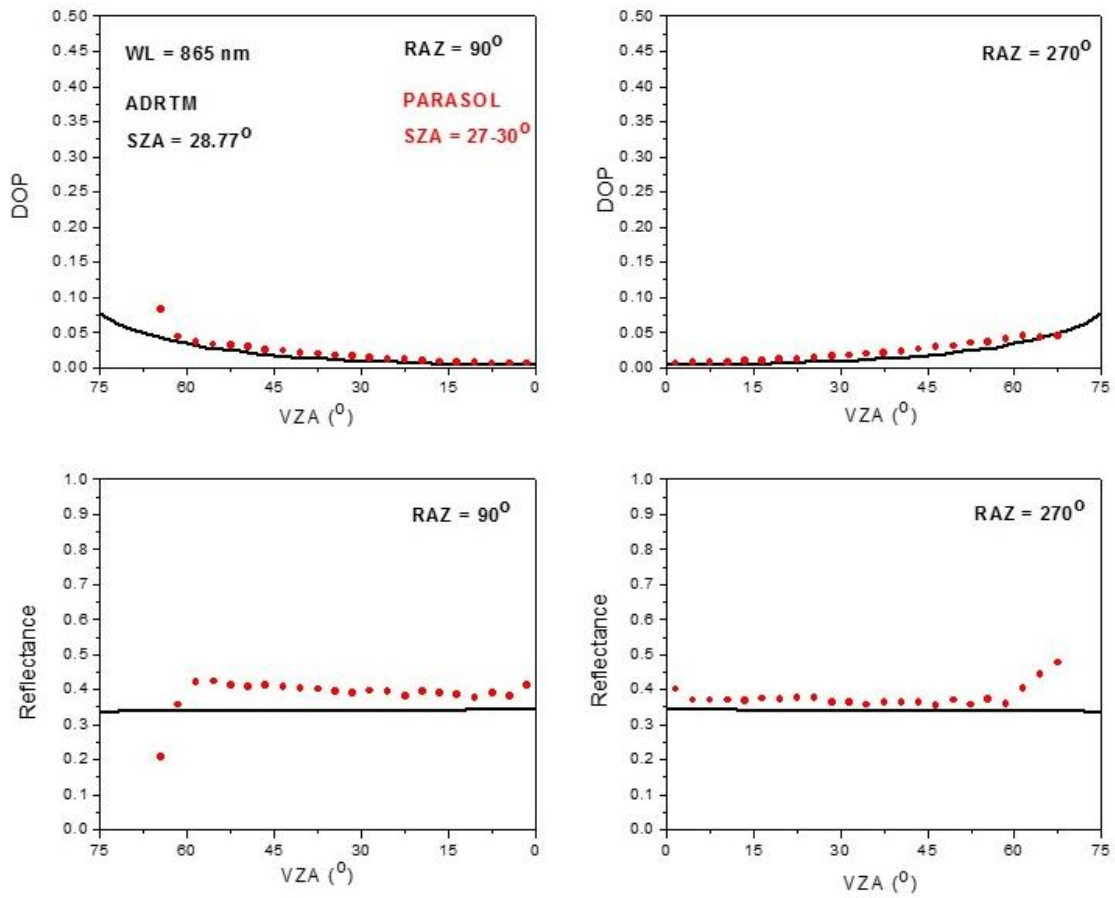
10  
11  
12  
13  
14  
15  
16



1  
2  
3  
4  
5  
6  
7  
8  
9

**Figure 14. Comparison of the modeled DOP and reflectance of desert-reflected solar light at relative azimuth angles (RAZ) of 0° and 180° with those from the PARASOL data at the wavelength of 865 nm. The solar zenith angle (SZA) is 28.77° in the modeling. The SZA is in the bin of 27-30° for the PARASOL data.**

1  
2  
3

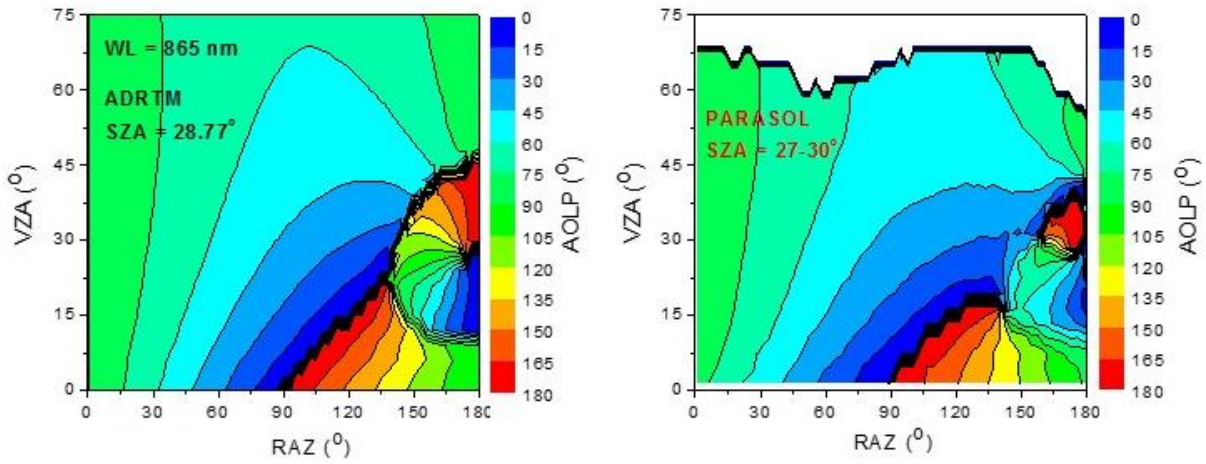


4  
5  
6  
7  
8  
9

Figure 15. Same as in Fig. 14, but at relative azimuth angles (RAZ) of 90° and 270°.

1

2



3

4

5 **Figure 16. Comparison of the modeled AOLP of desert-reflected solar light with those from**  
6 **the PARASOL data at the wavelength of 865 nm. The solar zenith angle (SZA) is 28.77° in**  
7 **the modeling. The SZA is in the bin of 27-30° for the PARASOL data.**

8

9

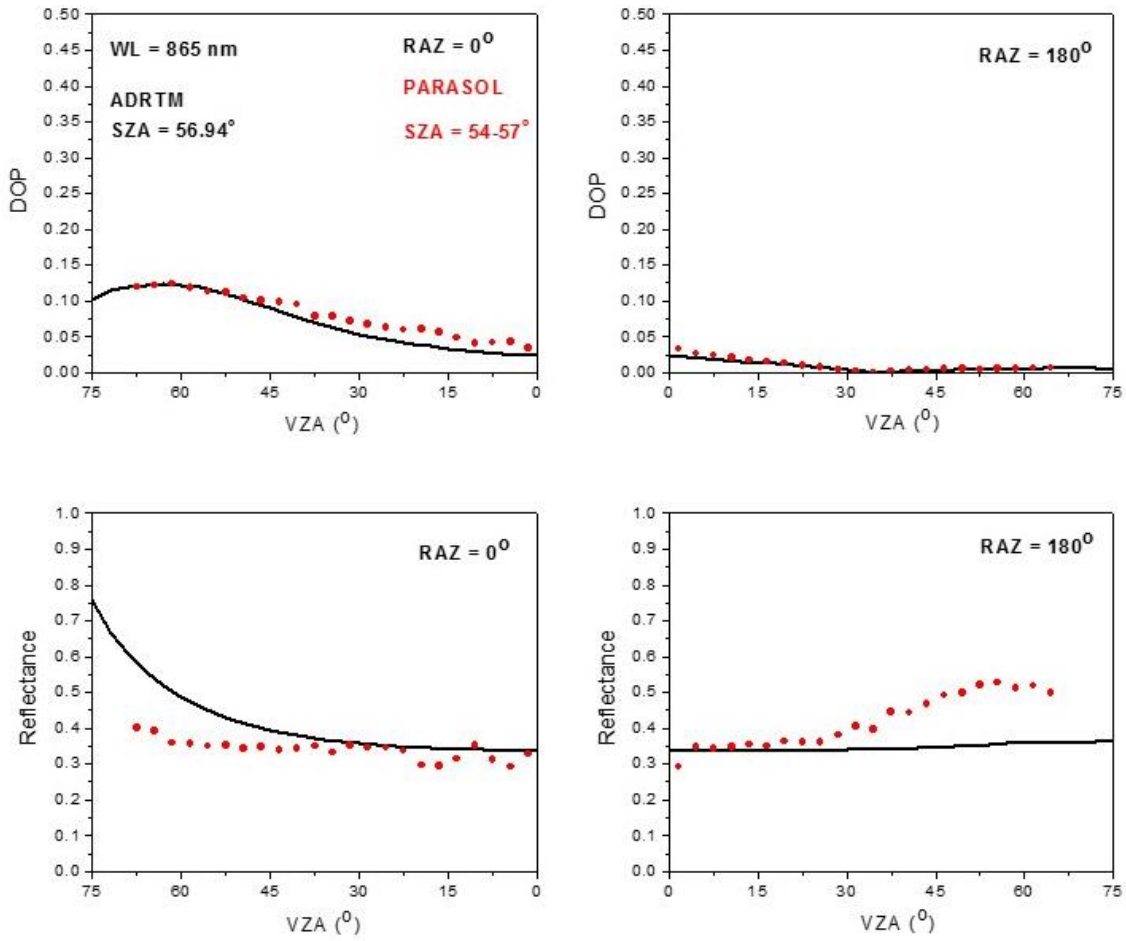
10

11

12

13

14



1

2

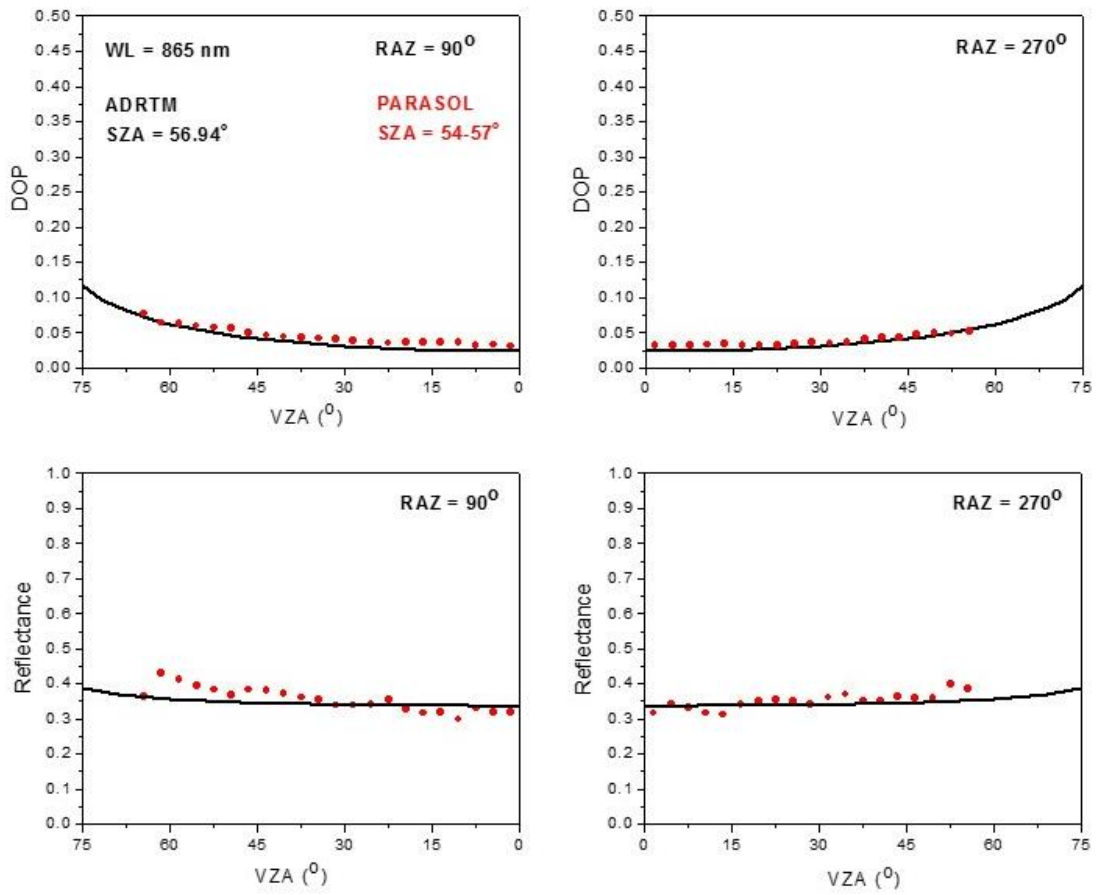
3 **Figure 17. Comparison of the modeled DOP and reflectance of desert-reflected solar light**  
 4 **at relative azimuth angles (RAZ) of 0° and 180° with those from the PARASOL data at the**  
 5 **wavelength of 865 nm. The solar zenith angle (SZA) is 56.94° in the modeling. The SZA is**  
 6 **in the bin of 54-57° for the PARASOL data.**

7

8

9

1



2

3

4 **Figure 18. Same as in Fig. 17, but at relative azimuth angles (RAZ) of 90° and 270°.**

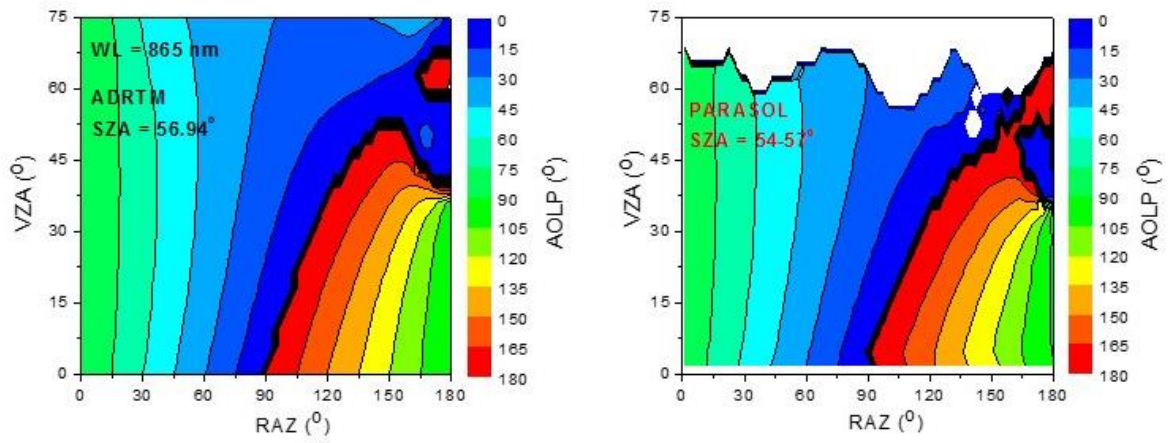
5

6

7

8

1



2

3

4 **Figure 19. Comparison of the modeled AOLP of desert-reflected solar light with those from**  
5 **the PARASOL data at the wavelength of 865 nm. The solar zenith angle (SZA) is 56.94° in**  
6 **the modeling. The SZA is in the bin of 54-57° for the PARASOL data.**

7

8

9

10

11

12

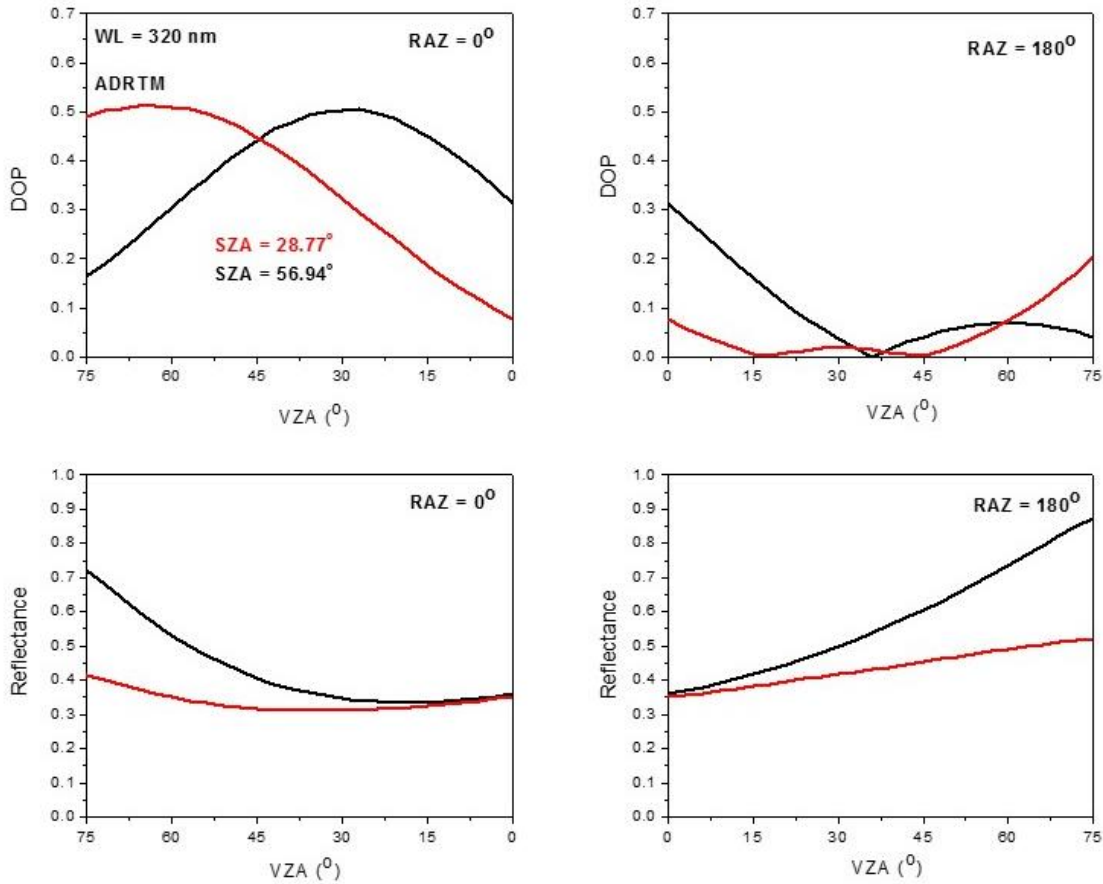
13

14

15

1

2



3

4

5

6 **Figure 20. The modeled DOP and reflectance of desert-reflected solar light at relative**  
7 **azimuth angles (RAZ) of 0° and 180° at the wavelength of 320 nm. The solar zenith angle**  
8 **(SZA) is 28.77° and 56.94°, respectively, in the modeling.**

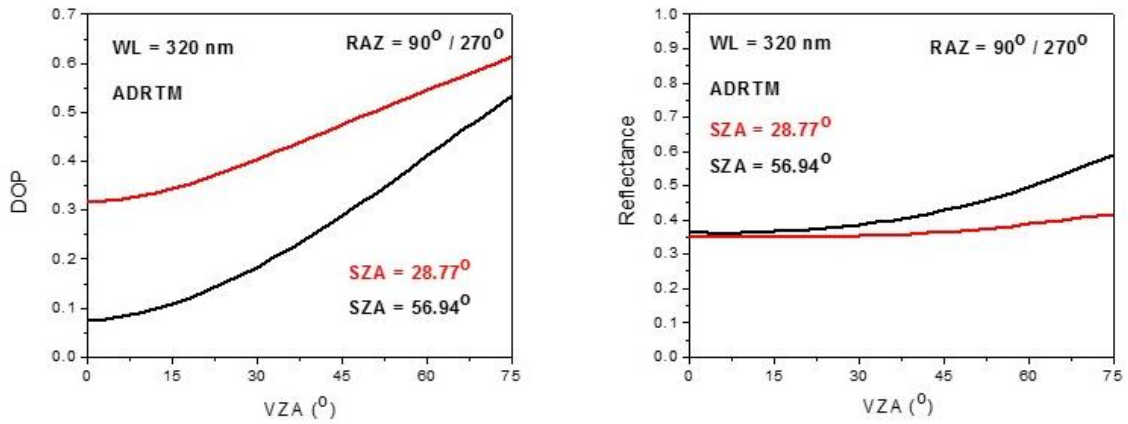
9

10

1

2

3



4

5

6 **Figure 21. Same as in Fig. 20, but at relative azimuth angles (RAZ) of 90° and 270°.**

7

8

9

10

11

12

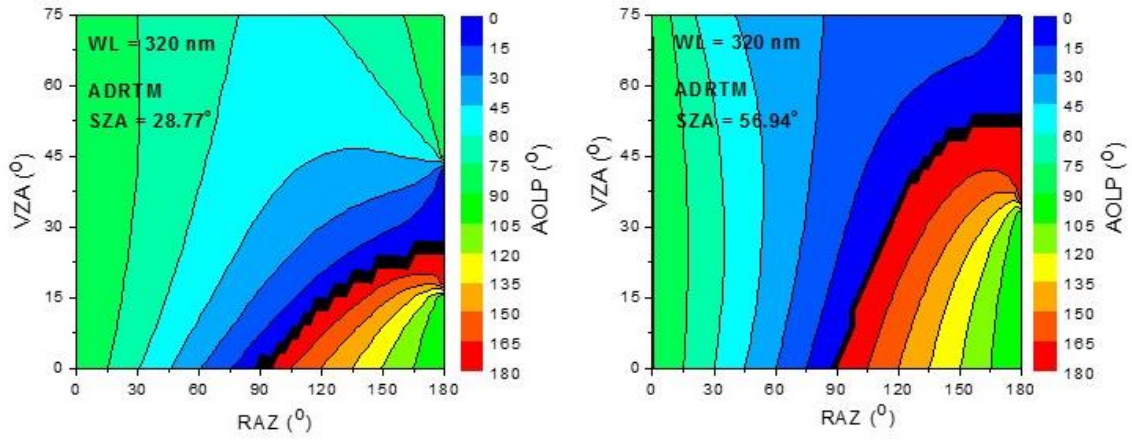
13

14

15

16

1



2

3

4

5 **Figure 22. The modeled AOLP of desert-reflected solar light at the wavelength of 320 nm.**

6 **The solar zenith angle (SZA) is 28.77° and 56.94°, respectively, in the modeling.**

7

8

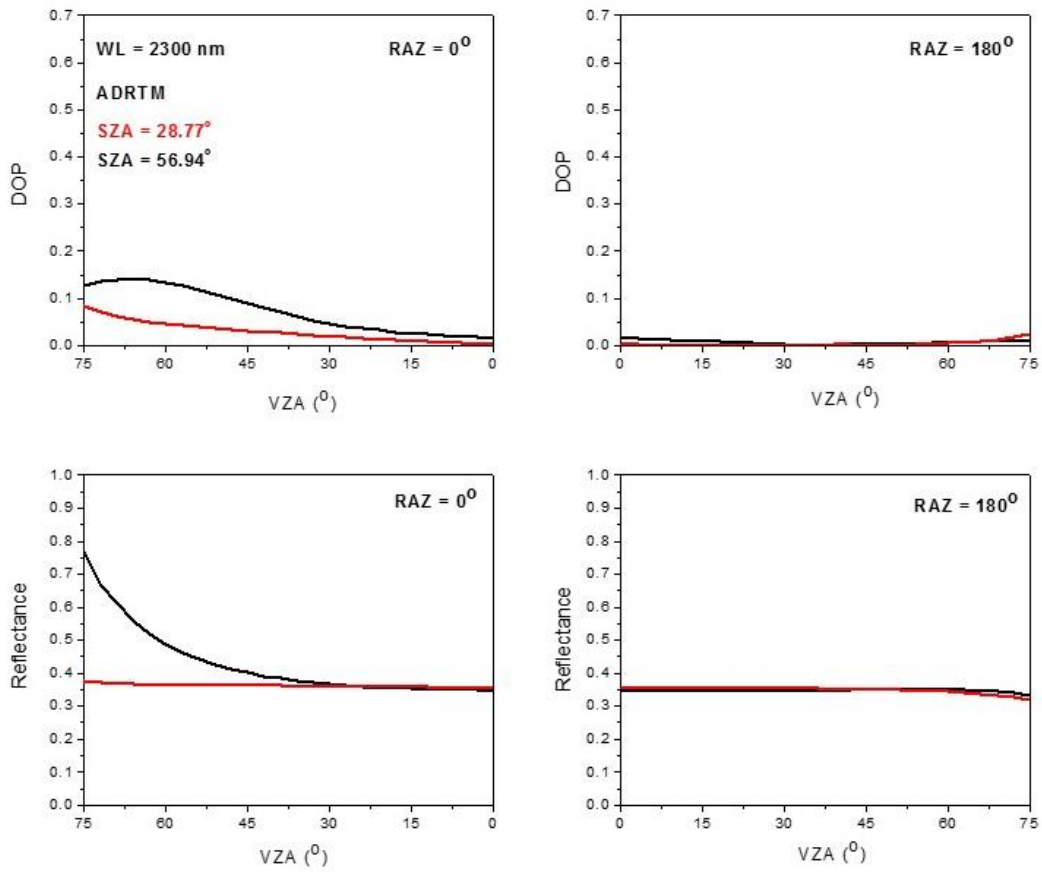
9

10

11

12

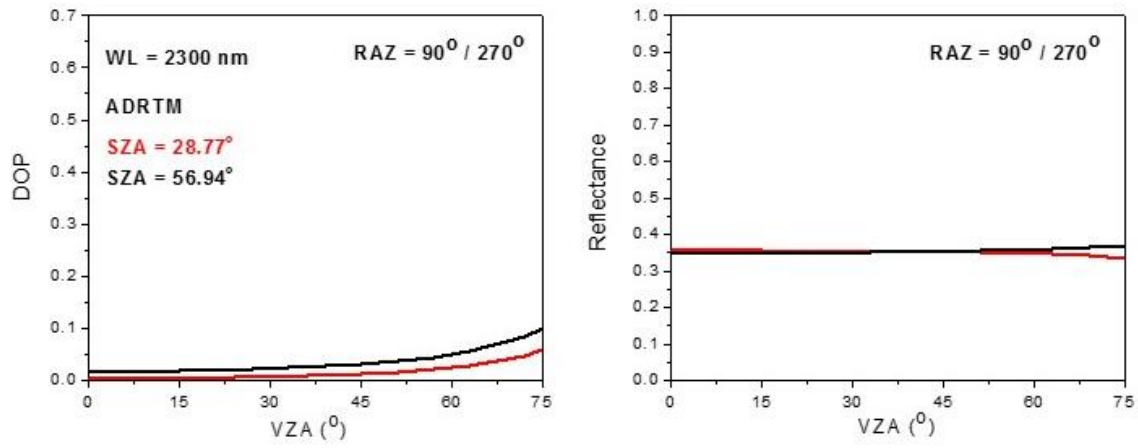
13



1  
2  
3  
4  
5  
6  
7  
8  
9  
10

**Figure 23. The modeled DOP and reflectance of desert-reflected solar light at relative azimuth angles (RAZ) of 0° and 180° at the wavelength of 2300 nm. The solar zenith angle (SZA) is 28.77° and 56.94°, respectively, in the modeling.**

1  
2  
3  
4

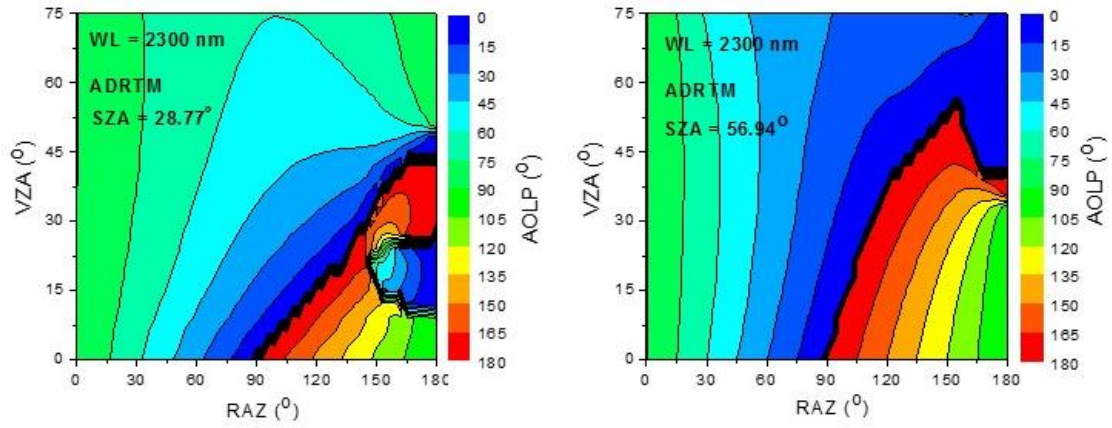


5  
6  
7  
8  
9  
10  
11  
12  
13  
14  
15  
16

Figure 24. Same as in Fig. 23, but at relative azimuth angles (RAZ) of 90° and 270°.

1

2



3

4

5 **Figure 25. The modeled AOLP of desert-reflected solar light at the wavelength of 2300 nm.**

6 **The solar zenith angle (SZA) is 28.77° and 56.94°, respectively, in the modeling.**

7